TEMPERATURE AND SALINITY STRUCTURE OF THE WINTERTIME BERING SEA MARGINAL ICE ZONE

by

John L. Newton

Science Applications, Inc.
1200 Prospect Street
La Jolla, California 92038

Final Report
Outer Continental Shelf Environmental Assessment Program
Research Unit 616

July 1982

ACKNOWLEDGMENTS

The winter 1980 CTD data were collected jointly by the Naval Postgraduate School and Science Applications, Inc., on the Winter 1980 Arctic West Cruise of the USCGC *Polar Star.*

The Arctic Submarine Laboratory of the Naval Ocean Systems Center, San Diego, CA, provided the icebreaker services and logistical support for the field measurements. The field work and preliminary analysis were also supported by Office of Naval Research Contract N00014-80-C-0368, with Science Applications, Inc., La Jolla, CA. This analysis and report were prepared under NOAA Contract NA81RAC00154.

ABSTRACT

Wintertime CTD sections across the Marginal Ice Zone (MIZ) of the Central Bering Sea shelf are analyzed and compared with fall CTD data. During the wintertime at depths shallower than 75 m, the water column was homogeneous and near freezing. Between the 75 and about 125 m isobaths, the structure was essentially two-layer with a cool-fresh upper layer overlying a warmer more saline bottom layer. Upper layer temperatures were significantly (>0.1°C) above freezing for a distance of 50-100 km into the ice pack. The horizontal temperature and salinity gradients are intensified during the winter in the region of the ice edge. Correspondingly, the baroclinic currents in the upper layer appear to be strengthened and to follow along the ice edge. Fall to March comparisons do not reflect total changes in heat and salt content in the MIZ over a season. The changes are investigated to identify the important ice-ocean interactions.

Changes in temperature and salinity between fall and winter in the region of the MIZ indicate a heat loss of about 3.7 x 10^4 cal/cm^2 of which 60-66% occurred in the upper layer and 34-40% in the lower layer; and reduction in salt content of 2.4 g/cm^2 with 54-56% in the upper layer and 44-46% in the lower layer. The changes in total heat and salt content can be attributed to a heat loss through the surface (85% of the total heat change) plus a heat loss (15% of the total) and freshening due to ice melt of about 1 maveraged over the 200 km MIZ. Regression analysis of heat and salt content change in 25 km intervals along the MIZ are consistent with the concept of a direct surface exchange of heat plus heat loss and freshening by ice melt. The slope of the regression (equivalent to ρL, the density ofice times the latent heat of fusion) averaged about 62 cal/cm^3; the intercept (equivalent to direct surface heat loss) was 3.1 x 10^4 [cal/cm^2] for the total heat loss and 2 x 10^4 [cal/cm^2] for the upper layer. Changes in the temperature and salinity of the upper layer were significantly correlated with a slope of $\cong$ 2.5°C/ppt, consistent with modification by ice melting. From fall to late March about 1 m of ice appears to have melted in the 200 kmwide MIZ. This is equivalent to a southward movement of 0.5 m thick ice into the MIZ at about 8 cm/sec over a two month period.

TABLE OF CONTENTS

LIST OF FIGURES

Figure *Page*

LIST OF TABLES

1. INTRODUCTION

During March 1980, Conductivity and Temperature versus Depth (CTD) profiles were obtained along two sections which crossed the Bering Sea Marginal Ice Zone (MIZ) over the southeastern and central shelf. Preliminary results from these measurements have been presented by Newton and Andersen, 1980 and Paquette and Bourke, 1980. These sections supplement the relatively meager data base presently available to study the physical oceanographic processes relevant to the characteristics of the wintertime Bering Sea MIZ.

The purpose of this report is to present a detailed analysis of these sections within the context of recent physical oceanographic studies of the Bering Sea MIZ. The structure and characteristics of these sections will be compared to that of some pertinent sections from other seasons. Finally, these analyses and comparisons will form the basis for a discussion of some potentially important physical oceanographic process in the Bering Sea MIZ.

2. OCEANOGRAPHIC BACKGROUND

Kinder and Schumacher, 1981a, described the hydrographic structure of the Southeastern Bering Sea Shelf, southeast of St. Matthew Island. They identified three domains on the shelf based on the vertical hydrographic structure (Figure 2.1). This brief summary, following Kinder and Schumacher, 1981a, particularly reflects summertime conditions. In the shallow coastal domain, depths less than 50 m, the vertical structure is homogeneous with very little vertical stratification. During the late summer, temperatures are usually high (8-12°C) and salinities are low (<31.5 ppt). The middle domain, between the 50 m and 100 m isobaths, is characterized by a two-layer structure with high stratification. Bottom temperatures remain cool (-1 to 3°C) throughout the summer and salinities are about 31.5 ppt. Lying seaward of the 100 m isobath, the outer domain has a three-layer structure, mixed surface and bottom layers and a stratified interior, with moderate stratification. Salinities in the outer domain are high, greater than 32 ppt and temperatures fall in the 3 to 6°C range. The three domains are separated

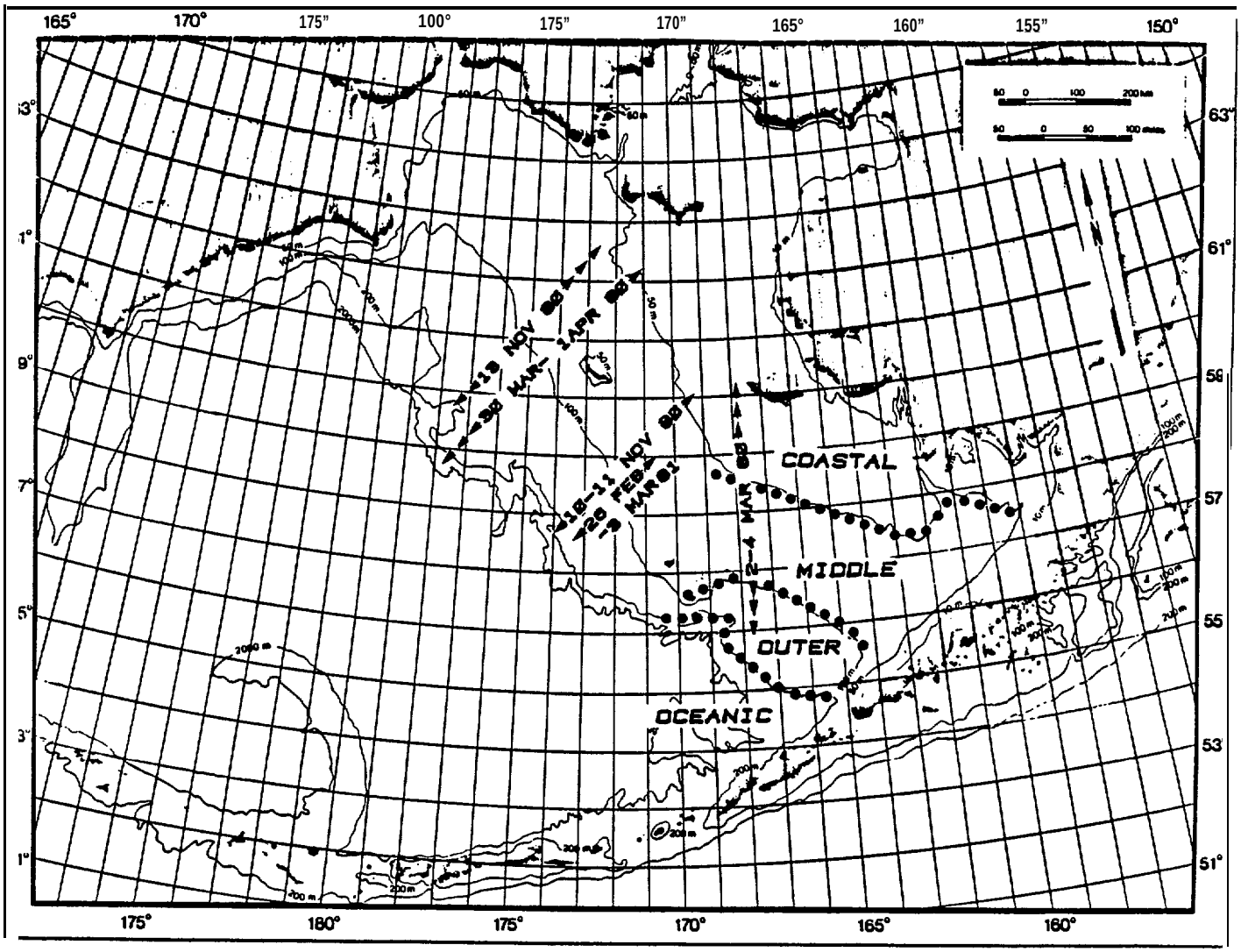

Figure 2.1. Location and orientation of CTD sections discussed in this report. The hydrographic domains of the southeastern Bering Sea Shelf from Kinder and Schumacher (1981a) are indicated.

by fronts, an inner front along the 50 m isobath, a middle front at about the 100 m depth contour and a shelf break front which separates the seaward extent of the outer domain from the oceanic waters of the deep Bering Sea.

Kinder and Schumacher, 1981a, identified several physical processes which act to form or alter the hydrographic structure over the shelf. Local changes in water mass characteristics can be caused by cooling and heating at the sea surface, evaporation and precipitation and the effects of ice melting and freezing. Because of the small mean flow on the shelf the impact of local processes are believed to be more important than changes due to advection. Vertical mixing due to tides and winds is one of the processes which determine the vertical hydrographic structure. In the coastal domain tide and wind stirring is sufficient to overcome buoyancy addition and thus maintain the vertically homogeneous structure. The deeper depths of the middle domain prevent tide and wind mixing from stirring the entire water column. The result is a wind stirred upper layer separated from a tidally mixed bottom layer by a sharp pycnocline region. In the outer domain the tide-mixed and wind-mixed layers do not meet thus leaving an interior stratified region.

Kinder and Schumacher, 1981a, indicate that during the winter, waters over most of the shelf are vertically homogeneous. They note two exceptions: warm saline water from the oceanic domain which intrudes onto the shelf along the bottom into the outer domain, and a low salinity lens of meltwater which can stratify the water.

The circulation over the southeastern Bering shelf (Kinder and Schumacher, 1981b) approximately corresponds to the hydrographic domains described above. In the outer regime (depths >100 m) the mean flow is about 1-5 cm/sec directed northwesterly along the isobaths and appears to be in geostrophic balance. The mean flow in the middle regime, between the 50 and 100 m depth contours, has a random direction and low speed (<0.5 cm/see). Near the inner front, along the 50 m isobath, the average circulation is in counterclockwise with speeds of 1-5 cm/sec. The majority (60 to 90%) of the horizontal kinetic energy over the shelf is tidal with 80% of this tidal energy in the semidiurnal band.

3. DATA

The Winter 1980 data were collected during the March 1980 Bering Sea Cruise of the USCGC POLAR STAR (Newton and Andersen, 1980). A total of 83 CTD stations were occupied, of which 29 (stations 3-16 and 67-83) were located in or near the MIZ and will be emphasized here. Table 3.1 lists the positions and the date-time of occupation for these stations. A Neil Brown CTD (MK 111 microstructure profiler) interfaced to a Hewlett Packard 9835B desktop calculator was used to collect the data. Nansen bottles were employed to obtain independent checks on temperature and salinity. Newton and Andersen, 1980, describe the data collection procedures and cruise operations in more detail.

CTD data appropriate for comparison to these winter 1980 transects were obtained by Muench, 1981. Five CTD sections selected for discussion are located in Figure 2.1 and listed below. For ease of reference they are identified by season (W = Winter, F = Fall) and year (1980 or 1981). In chronological order these sections are:

W-80A (Newton and Andersen, 1980): A north-south 1 ine of CTD stations across the southeastern Bering Sea Shelf MIZ.

W-80B (Newton and Andersen, 1980): A northeasterly tending CTD section across the central Bering Sea shelf MIZ northwest of St. Matthew Island.

F-80A (Muench, 1981): A northeasterly directed transect of CTD stations across the central Bering Sea shelf southwest of St. Matthew Island.

F-80B (Muench, 1981): A line of CTD stations across the central Bering Sea shelf nearly coincident with section W-80B.

W-81 (Muench, 1981): Wintertime CTD stations which repeated a part of the F-80A transect.

Table 3.1. Station Data for Winter 1980 CTD Observation

W-80A

STATION	POSITION		DATE	TIME(Z)	DEPTH(m)
1	54-20.0N	166-17.0W	29 FE5 80	0019	778
2	54-36.0	166-12.0		0236	403
3	56-15.0	167-16.0		1230	128
4	56-23.5	167.08.0		1502	112
5	56-30.0	167-12.0		1636	126
6	56-37.0	167-14.0		1720	102
7	56-47.5	167.20.0	29 FEB 80	1849	91
8	56-50.0	167-23.0	1 MAR 80	0054	82
9	57-01,0	167-30.4		0239	79
10	57-14.5	167-39.7		0625	77
11	57-35.7	167-55.0		1143	73
12	57-57.0	168-10.0	1 MAR 80	2038	72
13	58-30.0	168-16.0	3 MAR 80	0400	59
14	59-05.0	168-08.0	3 MAR 80	1830	42
15	59-36.0	168-10.0	3 MAR 80	2348	40
16	59-52.1	168-16.5	4 MAR 80	0406	37

W-80B

STATION	POSITION		DATE	TIME(Z)	DEPTH(m)
67	61-36.0	172-08.0	28 MAR 80	1915	58
68	61-19.0	172-52.0	29 MAR 80	2030	64
69	61-01.0	173-40.0	30 MAR 80	2002	65
70	60-42.0	174-25.0	31 MAR 80	1109	89
71	60-24.0	175-08.0	31 MAR 80	2111	108
72	60-03.5	175-57.5	1 APR 80	0514	126
73	60-01.0	176-04.0	1 APR 80	0621	128
74	59-54.0	176-30.0	1 APR 80	1553	133
75	59-49.0	176-30.0	1 APR 80	2025	139
76	59-45.0	176-35.0	2 APR 80	0028	137
77	59-42.0	176-45.0		0159	139
78	59-39.0	176-53.0		0412	151
79	59-33.0	177-02.0		0916	152
80	59-29.0	177-07.0		1031	149
81	59-26.0	177-14.0		1136	159
82	59-20.0	177-24.0		1327	170
83	59-16.0	177-45.0	2 APR 80	1537	278

4. ANALYSIS OF MARCH 1980 CTD SECTIONS

4.1 Introduction

In this section, the two March 1980 MIZ CTD transects will be described individually. As indicated above, the CTD transects will be identified by season and year. Thus W-80A and W-80B (winter, 1980) are the transects across the southeastern Bering shelf and central Bering shelf, respectively, that were obtained during March 1980.

The analysis for each cross section includes:

- A description of the vertical temperature and salinity structure,
- Calculation of the horizontal property gradients along the section,
- An analysis of the temperature-salinity correlations including their relationship to the freezing point,
- Calculation of stratification parameters, and
- A short summary discussion.

4.2 Section W-80A

Section W-80A was occupied during the period 29 February to 3 March 1980. This section crossed the southeastern Bering Sea shelf between the 125 and 50 m depth contours (Figure 2.1); and thus extended from the outer shelf hydrographic domain, across the middle shelf into the coastal domain (Kinder and Schumacher, 1981a). Vertical cross sections of temperature and salinity along the southward end of this transect are shown in Figures 4.1a and b. The ice edge was located between Stations 9 and 10 over water of about 80 m depth.

The vertical structure along section W-80A generally corresponded to the hydrographic domains described by Kinder and Schumacher, 1981a. Seaward of Station 7, the vertical temperature and salinity structure could be characterized as three layered; a nearly homogeneous surface layer and a mixed bottom layer which is occasionally warm and saline (Stations 3 and 4) due to

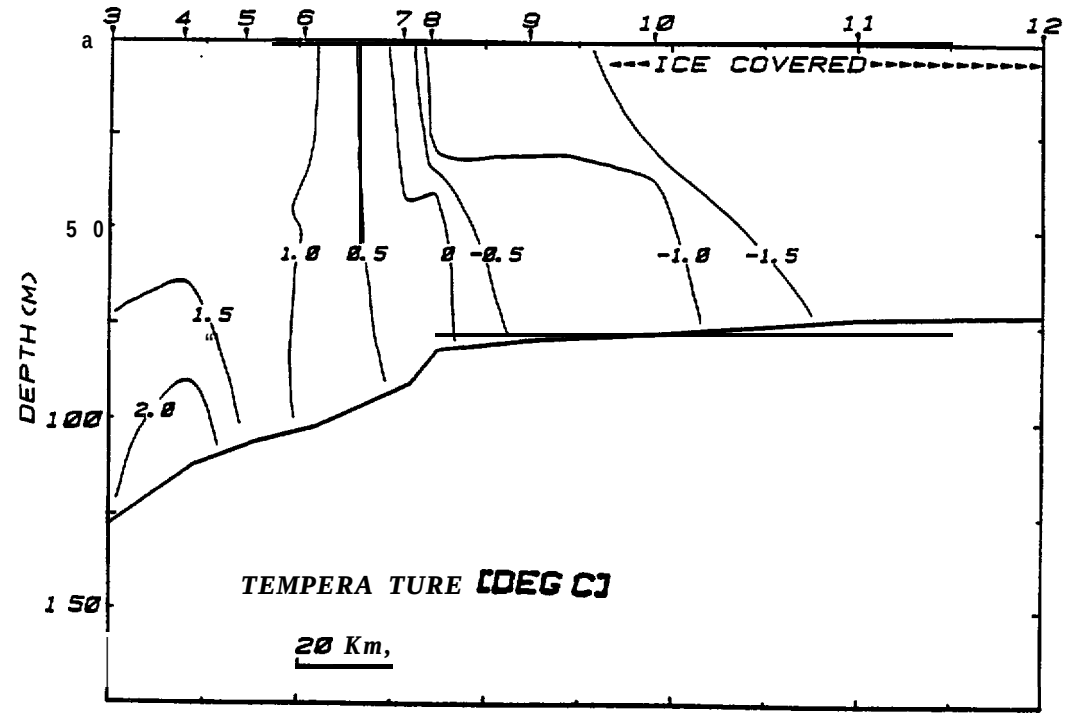

(a)

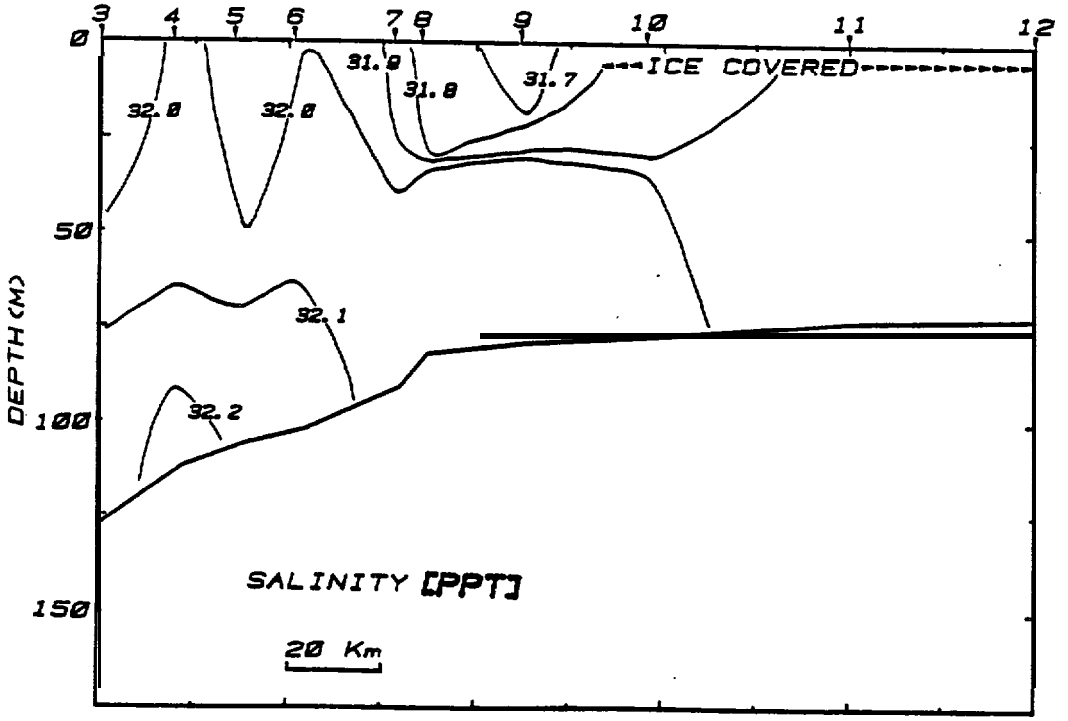

(b)

Figure 4.1. Vertical distribution of temperature (a) and salinity (b) across the southeastern Bering Sea shelf obtained during 29 Feb - 3 Mar 1980. W-80A.

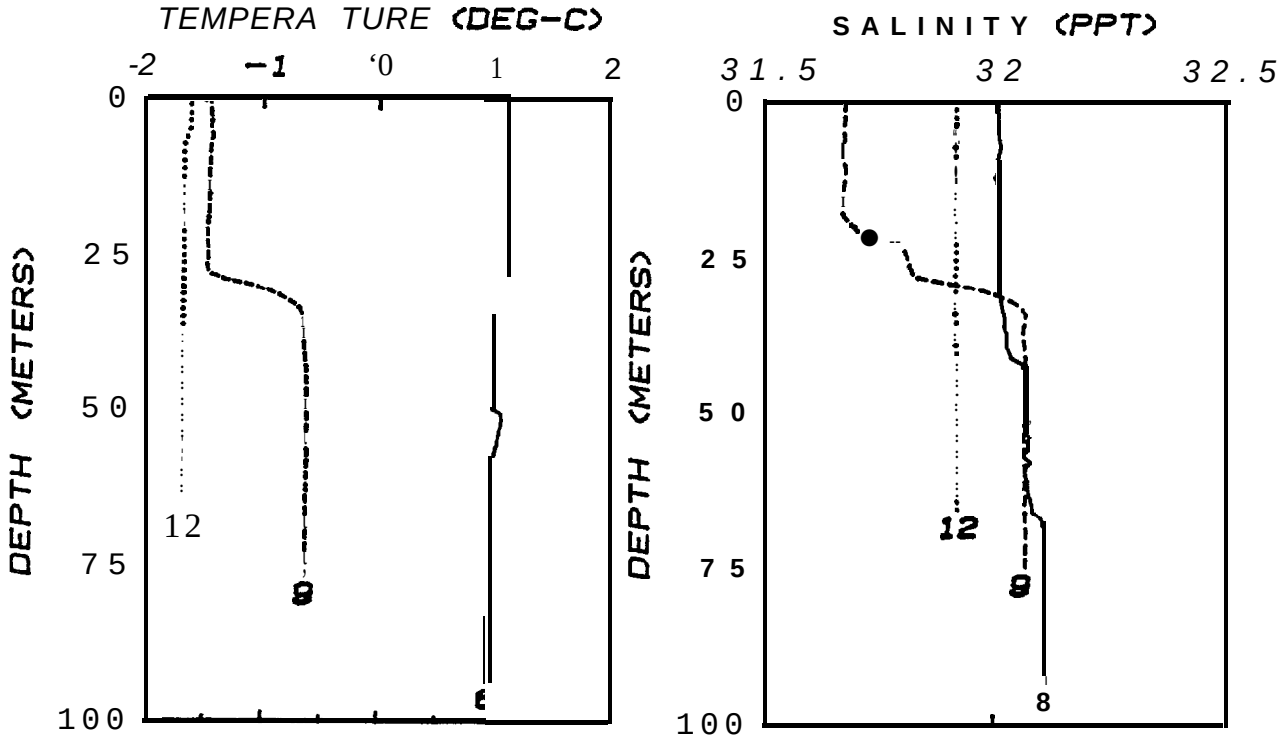

Figure 4.2. Vertical profiles of temperature and salinity at three representative stations along Section W-80A; Stations 6, 9 and 12.

an intrusion of Bering Sea water onto the shelf along the bottom, which were separated by middle layer which displayed small scale structure. This vertical structure (cf. Station 6, Figure 4.2) is typical of the outer-shelf domain (Kinder and Schumacher, 1981a). From Station 7 northward through Station 10, the vertical structure was two-layered (Station 9, Figure 4.2) corresponding to the middle shelf hydrographic domain. The vertical temperature and salinity distributions at Station 11 and northward were essentially vertically homogeneous (Station 12, Figure 4.2) characteristic of the coastal domain.

The surface- and bottom-layer temperature and salinity are plotted versus distance along the section in Figure 4.3. The transition from the three-layer outer- to the two-layer middle-shelf domains occurred between Stations 6 and 7 within a few km of the 100 m contour, The transition from the middle-shelf to the vertically homogeneous coastal structure occurred between Stations 10 and 11, about 100 km north of the 100 m contour in water

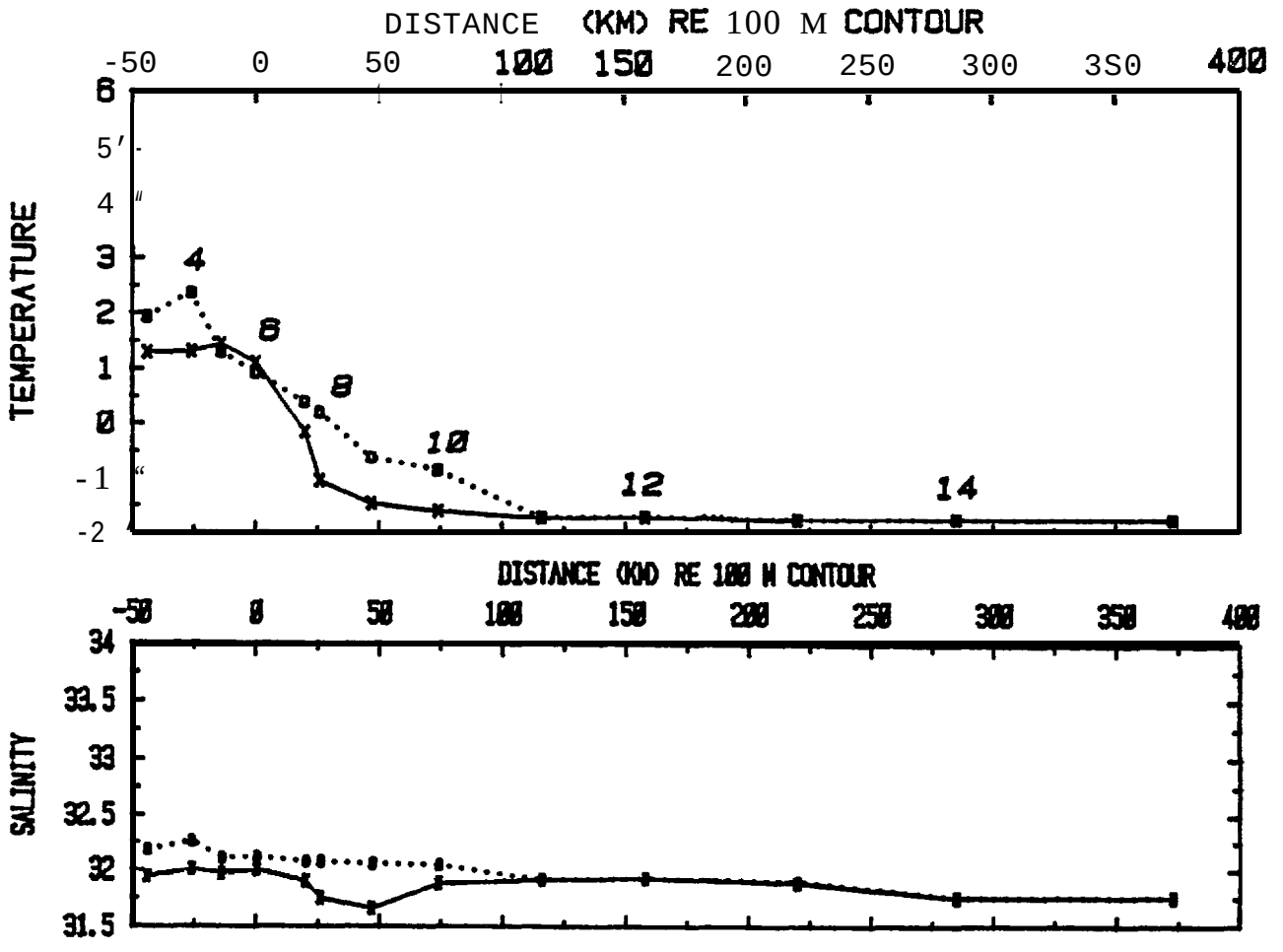

Figure 4.3. Section W-80A. Surface (x–x) and lower (0···0) layer temperature (°C) and salinity (ppt) versus distance (km) along section W-80A relative to the 100 m isobath.

of 75 m depth. In the upper layer temperature decreased from +1.4°C to <-1.5°C over a 60 m distance between Stations 5 and 9 (a regression slope of -5.3 x 10^{-2}°C/km) with a corresponding salinity decrease from 32.0 ppt to 31.7 ppt (a regression slope of -6 x 10-3ppt/km). In the lower layer, property changes along the section were more gradual. Between Station 3 and 11, a distance of 160 km temperature decreased nearly linearly from +2.0°C to <-1.5°C(a regression slope of -2.6 x 10^{-2}°C/km) while salinity decreased from 32.2 ppt to 31.9 ppt (a regression slope of -2 x 10^{-3} ppt/km).

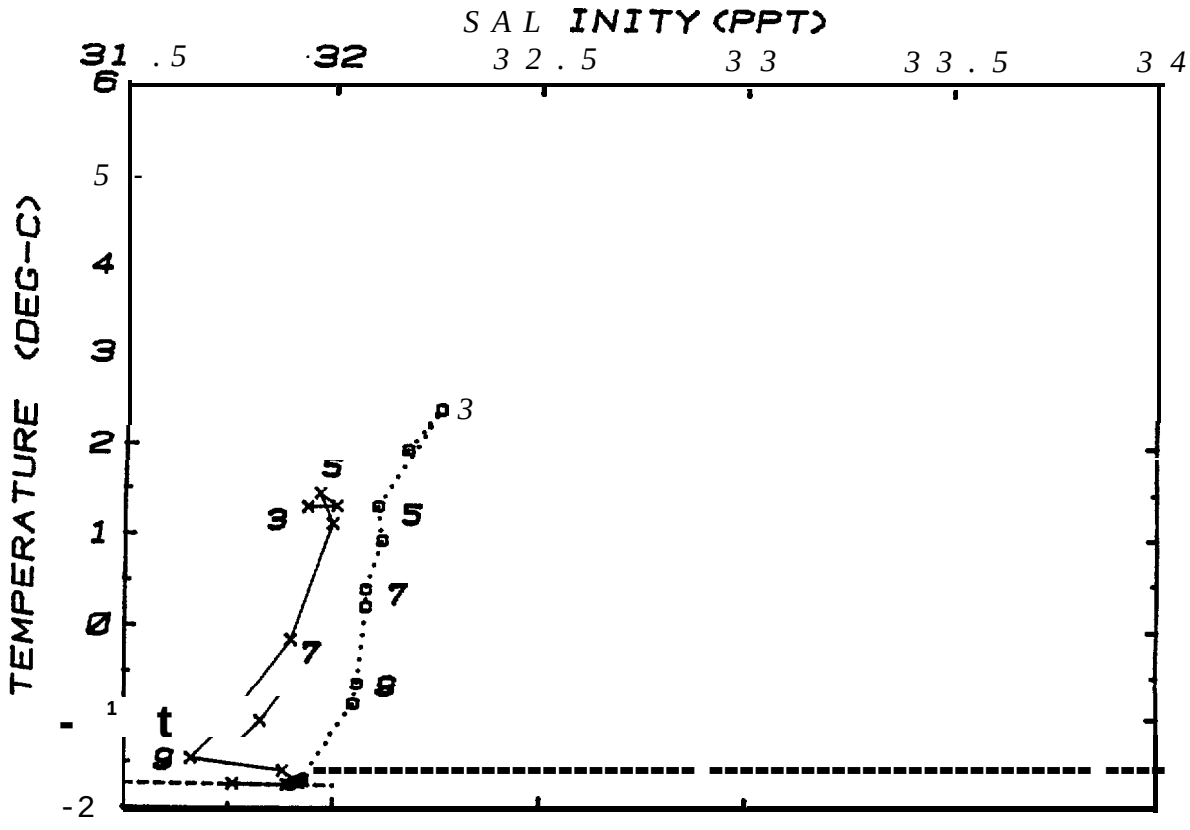

Figure 4.4. Temperature - salinity characteristics along Section W-80A plotted in the T-S plane proceeding from open water northward for upper (x–x) and lower (0···0) layer.

Figure 4.4 compares the temperature and salinity characteristics of the upper and lower layers along the section in the T-S plane. Progressing from the outer shelf through the middle shelf domain, the lower layer cools *to* the freezing point and freshens along a nearly linear T-S correlation (with a regression slope of $\frac{dT}{dS}$ = 13.6). The T-S correlation for the upper layer has an inflection point at Station 9. Seaward of this point (Stations 5-9) the T-S correlation has a slope of dT/dS = 8.5; while northward to Station 11 the slope is ∿-1.

Figure 4.5 shows the temperature of the upper and lower layers relative to the freezing "point calculated from the observed salinity using the formula of Doherty and Kester, 1974. It is interesting to note that the upper layer temperature is above the freezing point well in under the ice edge, at least to Station 10 and perhaps north of this.

The degree of vertical stratification was estimated as

$$\Delta\sigma_t \simeq \beta\Delta S - \alpha\Delta T \ , \qquad (1)$$

where

$\Delta\sigma_t$ = Sigma-T difference between upper and lower layer,

ΔS = Salinity difference between upper and lower layer,

ΔT = Temperature difference between upper and lower layer,

$$\beta = \frac{1}{\sigma t}\frac{\partial \sigma t}{\partial S} \simeq + 0.80 \text{ ppt}^{-1} \ , \text{ and}$$

$$\alpha = \frac{-1}{\sigma t}\frac{\partial \sigma t}{\partial T} \simeq + 0.053^{o}C^{-1} \ .$$

In the outer shelf domain vertical stratification (Figure 4.6) was about .10 to .20 σt units, and generally decreased toward the north. Within the middle shelf domain, stratification increased to $\sim$.3 σ_T units due to the freshening in the upper layer at Stations 7 through 10 (Figures 4.3 and 4.4). At Station 11 and northward vertical stratification was essentially zero.

4.3 Section W-80B

Section W-80B was occupied during 30 Mar - 2 Apr 80. This section crossed the central Bering Sea shelf from the 170 m contour northward to a water depth of about 70 m. The ice edge was located at Station 79 over water of about 150 m depth. Vertical distributions of temperature and salinity along this transect are shown in Figures 4.7a and b.

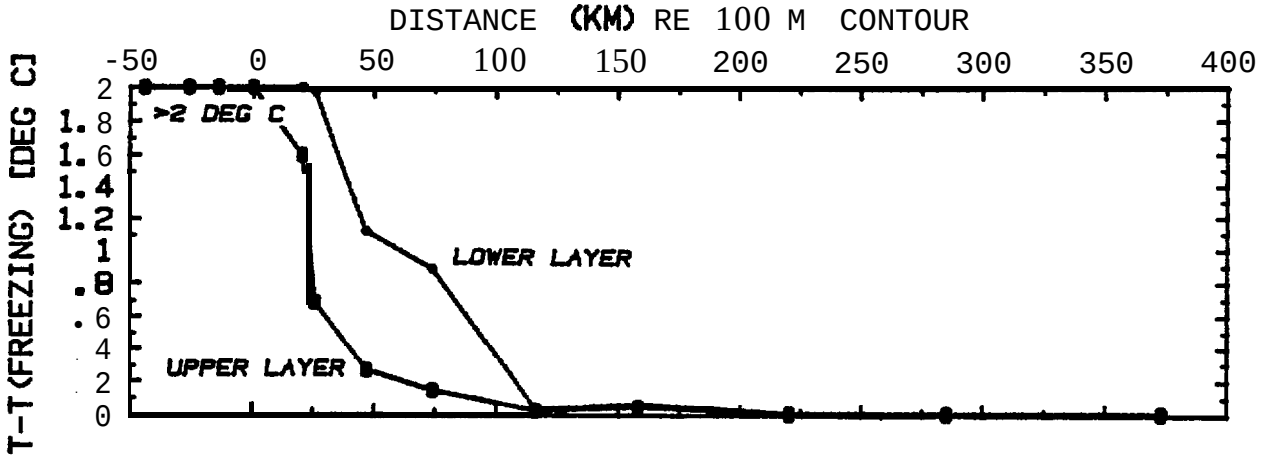

Figure 4.5. Upper (o-o) and lower (*···*) Iayer temperatures expressed as the departure from the freezing point (Doherty and Kester, 1974) versus distance (km) along Section W-80A relative to the 100 m isobath.

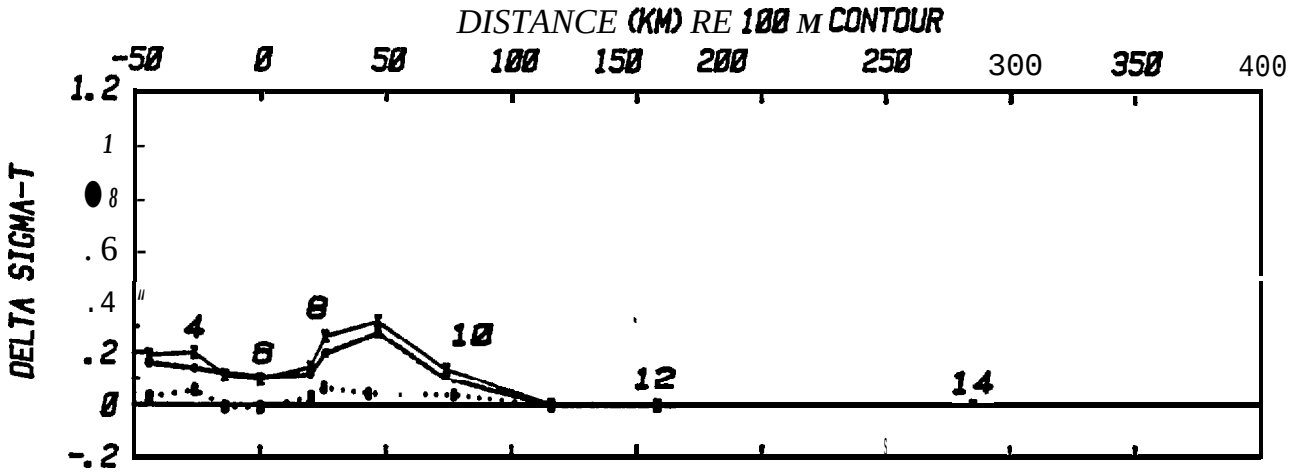

Figure 4.6. Section W-80A, vertical stratification versus distance (km) along the section relative to the 100 m isobath. The individual components, aAT (O···O) and βΔS (X-X) as well as the total stratificationβΔS-αΔT are plotted in units of sigma-T.

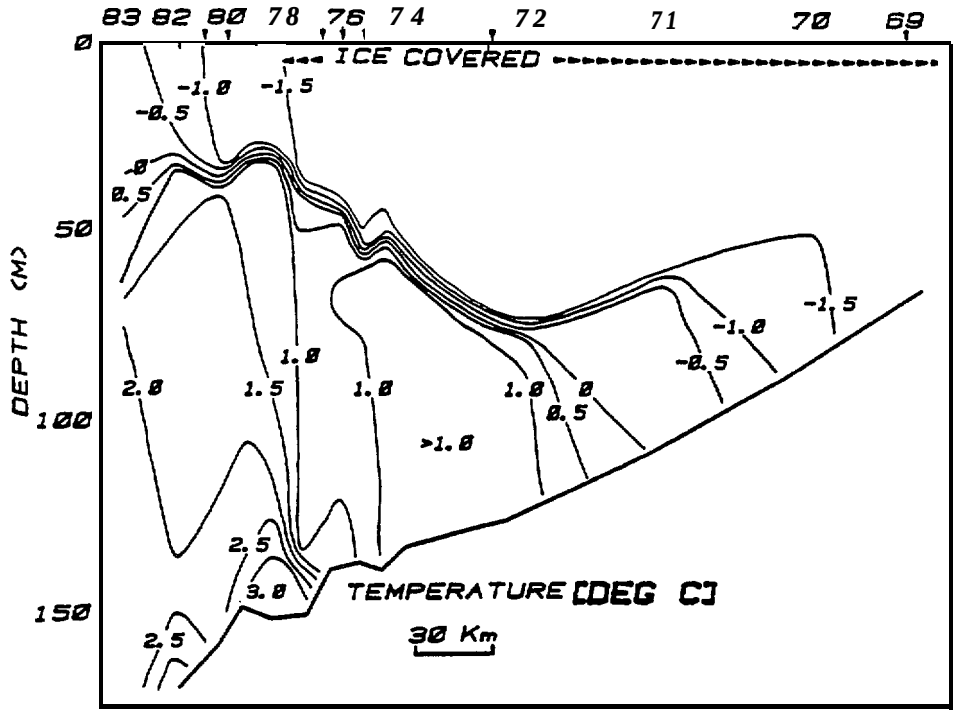

(a)

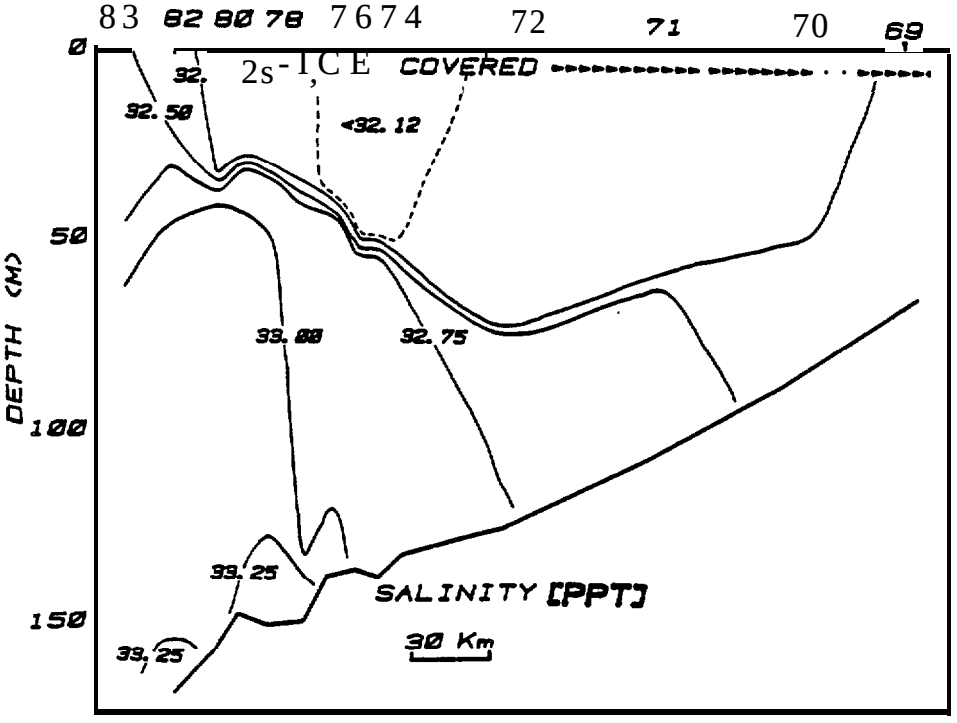

(b)

Figure 4.7. Vertical distribution of temperature (a) and salinity (b) across the central Bering Sea Shelf obtained during 30 Mar - 2 Apr 1980. W-80B .

The vertical structure along Section W-80B northward of the 125 m depth contour was analogous to that of Section W-80A described above. At Station 69 and northward in water depths of ~70 m, the water column is nearly homogeneous in temperature with minimal stratification ($\Delta\sigma_{t_c} \sim 0.05$) as shown by the profile at Station 68 (Figure 4.8). At Stations 70-73, bounded by the 75 and 125 m depth contours, the vertical structure was 2-layer with a 50 to 70 m thick homogeneous layer of cool fresh water overlying a warmer more saline layer which extended to the bottom (profile 72, Figure 4.8). Seaward of Station 73 over water depths greater than 125 m, the vertical structure became very complex but generally can be characterized as;

- A relatively cool, homogeneous surface layer which extended from Station 74 seaward about 60 km to Station 82. Progressing toward open water this layer thinned from 50 to 25 m, warmed from -1.6°C to -1.3°C, and increased in salinity from ~32.1 to >32.2 ppt. Below the homogeneous surface layer was a pycnocline of 10-20 m thickness across which the majority of the vertical temperature and salinity change occurred.
- Extending from the base of the pycnocline, at a depth of 40-60 m, to depths of 80-120 mwas a layer displaying temperature and salinity structure which consisted of small vertical scale (few m's) temperature minima/maxima with amplitudes of a few tenths of a degree centigrade.
- A nearly homogeneous layer with temperature of about 1°C extended from the base of the small-scale structure layer to the bottom at Stations 74-76 and to about 130 m at Stations 77 and 78.
- At the extreme south end of the section (at StatIons 77-83) a warm (>3.0°C) saline (>33.5 ppt) layer of about 20 m thickness extended into onto the shelf along the bottom.

Figure 4.9 plots the surface and bottom layer temperature and salinity versus distance along the section. The transition from essentially homogeneous to the two-layer structure occurred near Station 69, about 50 km north of the 100 m curve in about 70 m of water. The transition from a simple two-layer

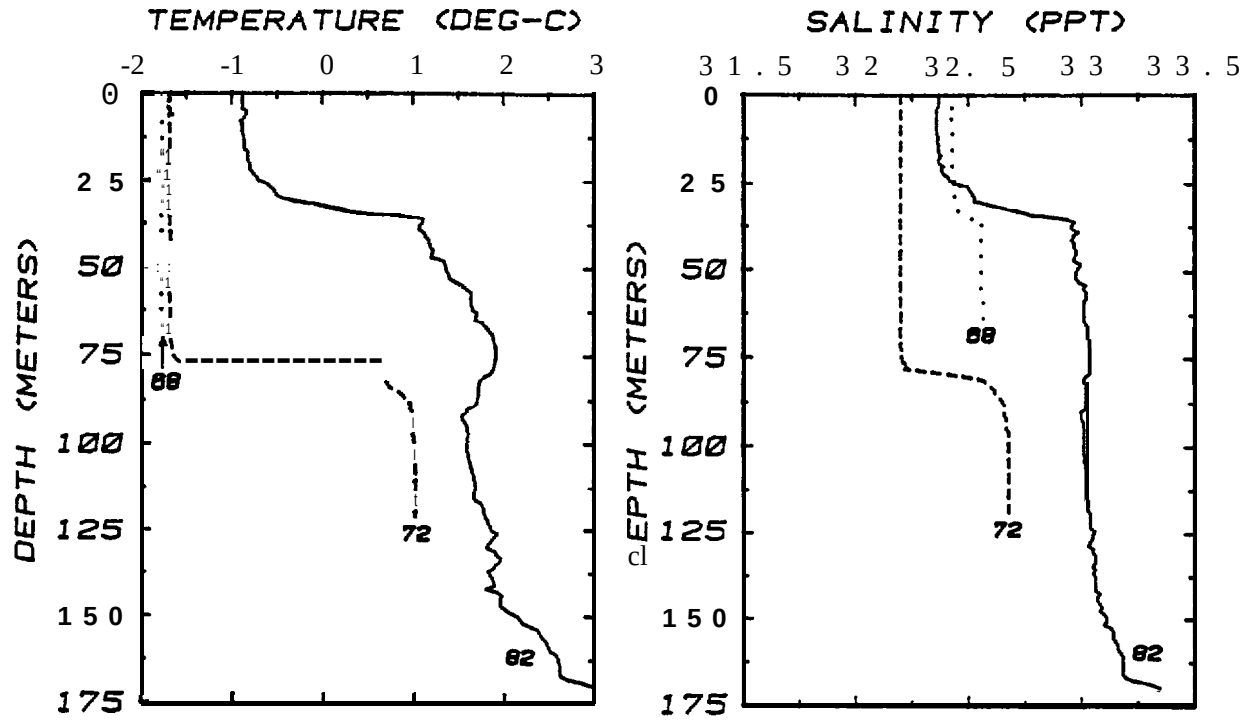

Figure 4.8. Vertical profiles of temperature and salinity at three representative stations along Section W-80B; Stations 82, 72 and 68.

system to the complex multilayer structure at the seaward end of the section took place near Station 74, 150 km seaward of the 100 m isobath. Upper layer temperature decreased from w- .4 to <-1.5°C between Stations 83 and 77 a distance of 74 km (a regression slope of -1.6 x 10^{-2}°C/km) with the corresponding salinity decreasing from 32.6 to 32.1 ppt (a slope of -6 x 10^{-3} ppt/km). The lower layer evidenced a greater total change in temperature and salinity along the section than the upper layer, however the changes took place over a greater distance (250 km from Station 83 to Station 70), thus the horizontal gradients, $\frac{dS}{dX}$ = -4 x 10^{-3}°C/km and $\frac{dT}{dX}$ = -1.9 x 10^{-2}°C/km were similar.

The T-S characteristics of the surface and bottom layer along section W-80B are shown in Figure 4.10. Between stations 83 and 77, the surface

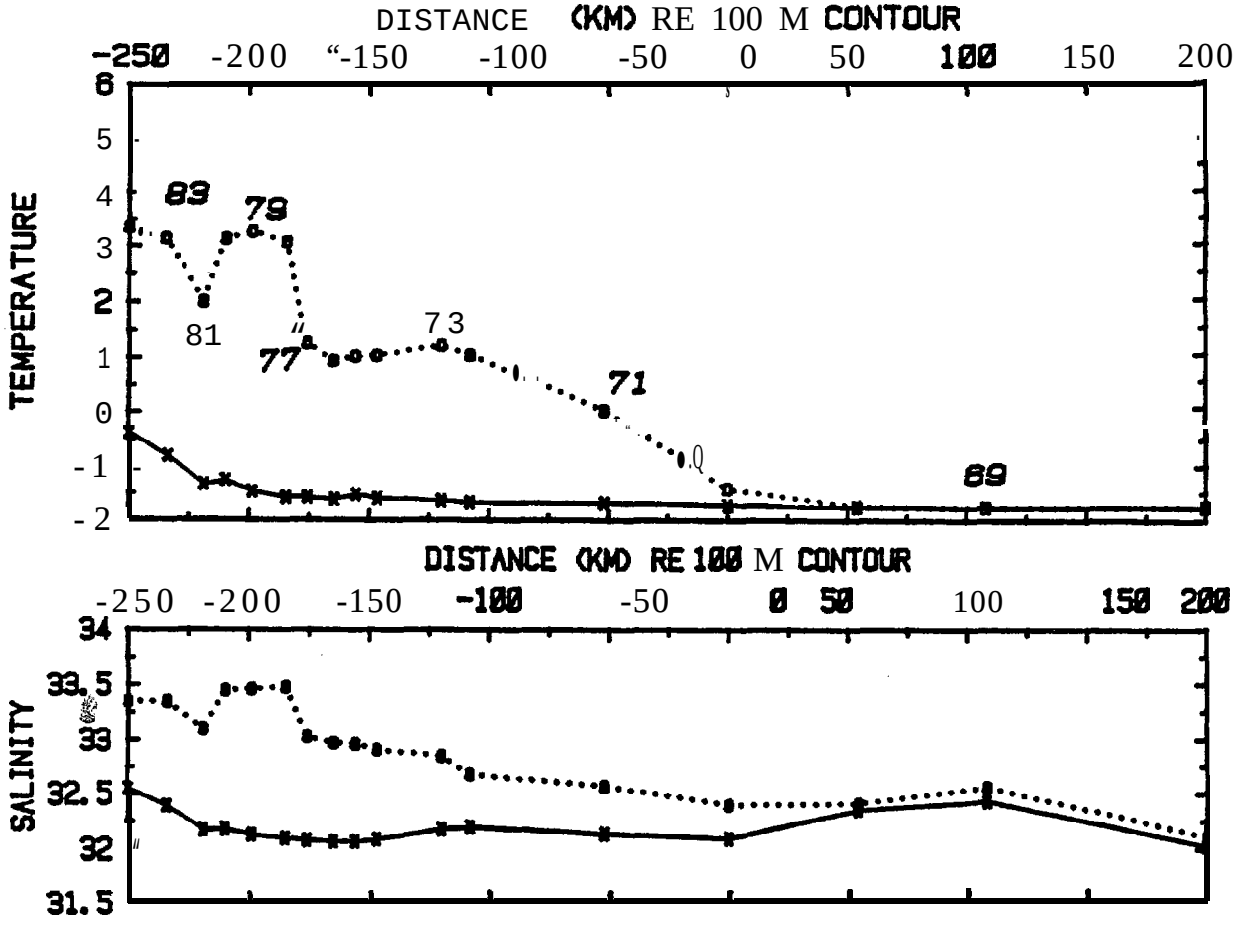

Figure 4.9. Surface (x-x) and lower (0-..0) 1 ayer temperature (°C) and salinity (ppt) versus distance (km) along Section W-80B relative to the 100 m isobath.

layer cools and freshens along a nearly linear T-S correlation with a regression slope $dT/dS = +2.6^{o}C/ppt$. The slope of the T-S correlation for the lower layer, Stations 70 through 83, is about $4.0^{o}C/ppt$.

The surface and bottom layer temperature, relative to the freezing point (Doherty and Kester, 1974), are plotted in Figure 4.11. The surface layer remained greater than $.1^{o}C$ above freezing for a distance of 100 km under the ice to Station 72. At Station 68 and northward, in the nearly vertically homogeneous region, both near-surface and near-bottom waters were essentially at the freezing point.

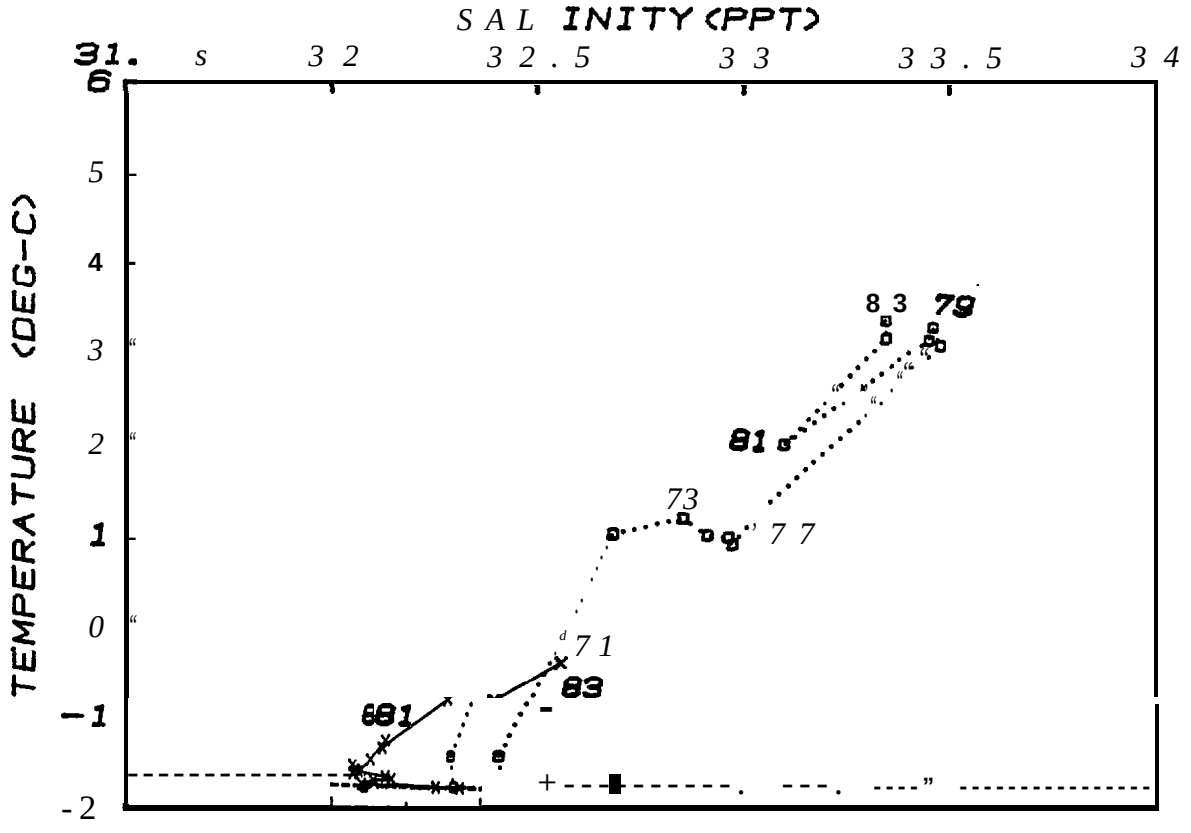

Figure 4.10. Temperature-salinity characteristics along Section W-80B plotted in the T-S plane proceeding from open water northward for the upper (x-x) and lower (0···0) layer.

Figure 4.12 plots the vertical density stratification along the section, computed by Equation (l), along with individual contributions to the density of the vertical temperature and salinity changes. Both temperature and salinity increased with depth at all stations along the section, thus the vertical salinity gradient, the major contributor, tended to stabilize the water column while the lesser effect of the vertical temperature gradient was destabilizing. The total density stratification was greatest ($\sim$0.8 σ_t units) near the ice edge due to relatively high bottom layer salinities and perhaps coincidentally a slightly freshened surface layer. Northward, through the two-layer region, density stratification decreased to a minimum 50 km north of the 100 m contour at Station 69.

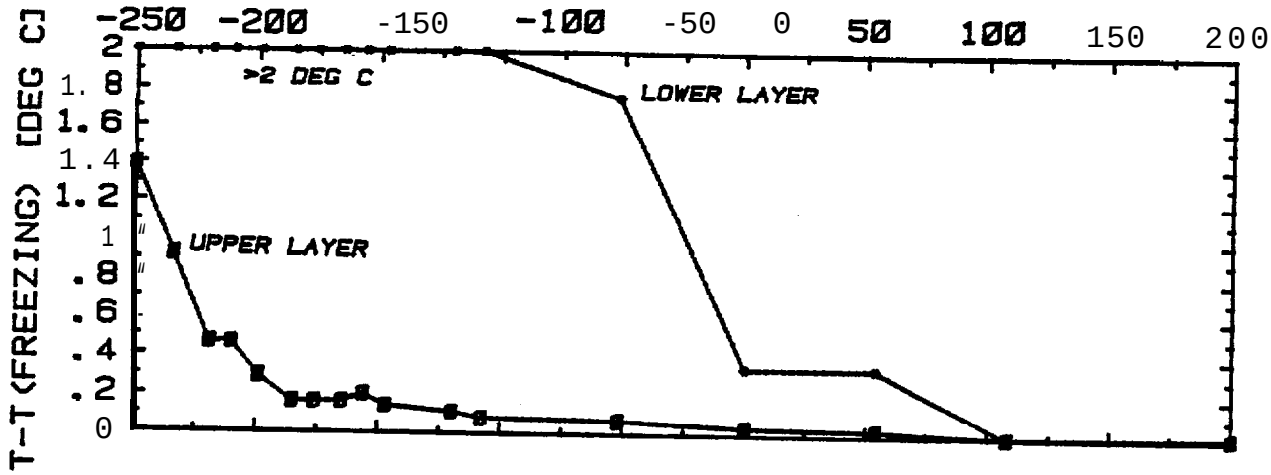

Figure 4.11. Upper (o-o) and lower (*...*) layer temperatures, expressed as the departure from the freezing point (Doherty and Kester, 1974) versus distance (km) along Section W-80B relative to the 100 m isobath.

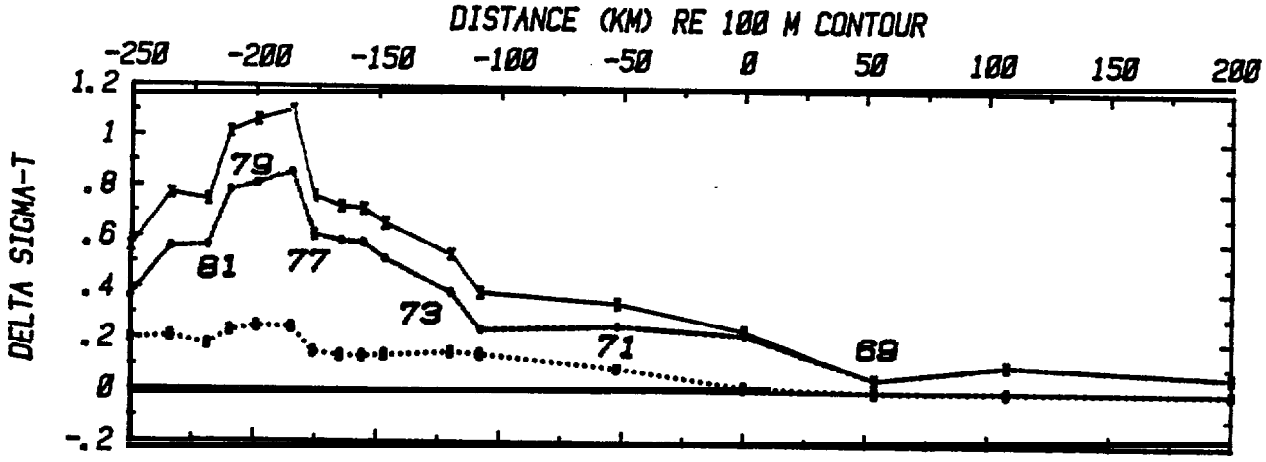

Figure 4.12. Vertical stratification versus distance (km) along Section W-80B relative to the 100 m isobath. The individual components $\alpha\Delta T$ (O···O) and $\beta\Delta S$ (x–x) as well as the total stratification, $\beta\Delta S$-$\alpha\Delta T$ are plotted in units of Sigma-T.

5. COMPARISONS WITH FALL 1980, WINTER 1981 CTD SECTIONS

5.1 Fall 1980, Winter 1981 CTD Sections

This section briefly describes the structure and T-S characteristics of the fall and winter data collected in 1980 and 1981 (Muench, 1981) in a format similiar to Section 4. These results will be used in later sections to describe the regional wintertime structure and compare fall to winter conditions.

- F-80A. The F-80A section crossed the central shelf southwest of St. Matthew Island (Figure 2.1). The vertical distribution of temperature, salinity and density (sigma-t) for this section has been described by Muench (1981). The water column was essentially two-layer with an interface at 50 to 60 m depth. Upper and lower layer temperature (°C) and salinity (ppt) versus distance along the section are shown in Figure 5.1. Upper and lower layer temperature decrease from 4°C near the shelf break northward to a minimum near Stations 7 and 8. Salinity decreases monotonically toward the north. From Station 1, north to Station 8, the horizontal gradients of temperature and salinity in the lower layer (-1.3×10^{-2}°C/km and -5×10^{-3} ppt/km) were slightly greater than corresponding upper layer gradients (-1.0×10^{-2}°C/km and -3×10^{-3} ppt/km). Stratification decreased from 0.4 sigma-t units at Station 1 to essentially 0 at Station 9 and northward (Figure 5.2) with both temperature (decreasing with depth) and salinity (increasing with depth) acting to stabilize the water column.

  The temperature-salinity characteristics of the upper and lower layers proceeding from deepwater northward are shown in Figure 5.3. Seaward of Stations 7 and 8, the T-S slope was positive ($\frac{dT}{dS}$ = +2.8°C/ppt for upper and +2.6°C/ppt for lower layer). North of Station 8 the slope was negative, $\frac{dT}{dS}$ = -1.2°C/ppt.

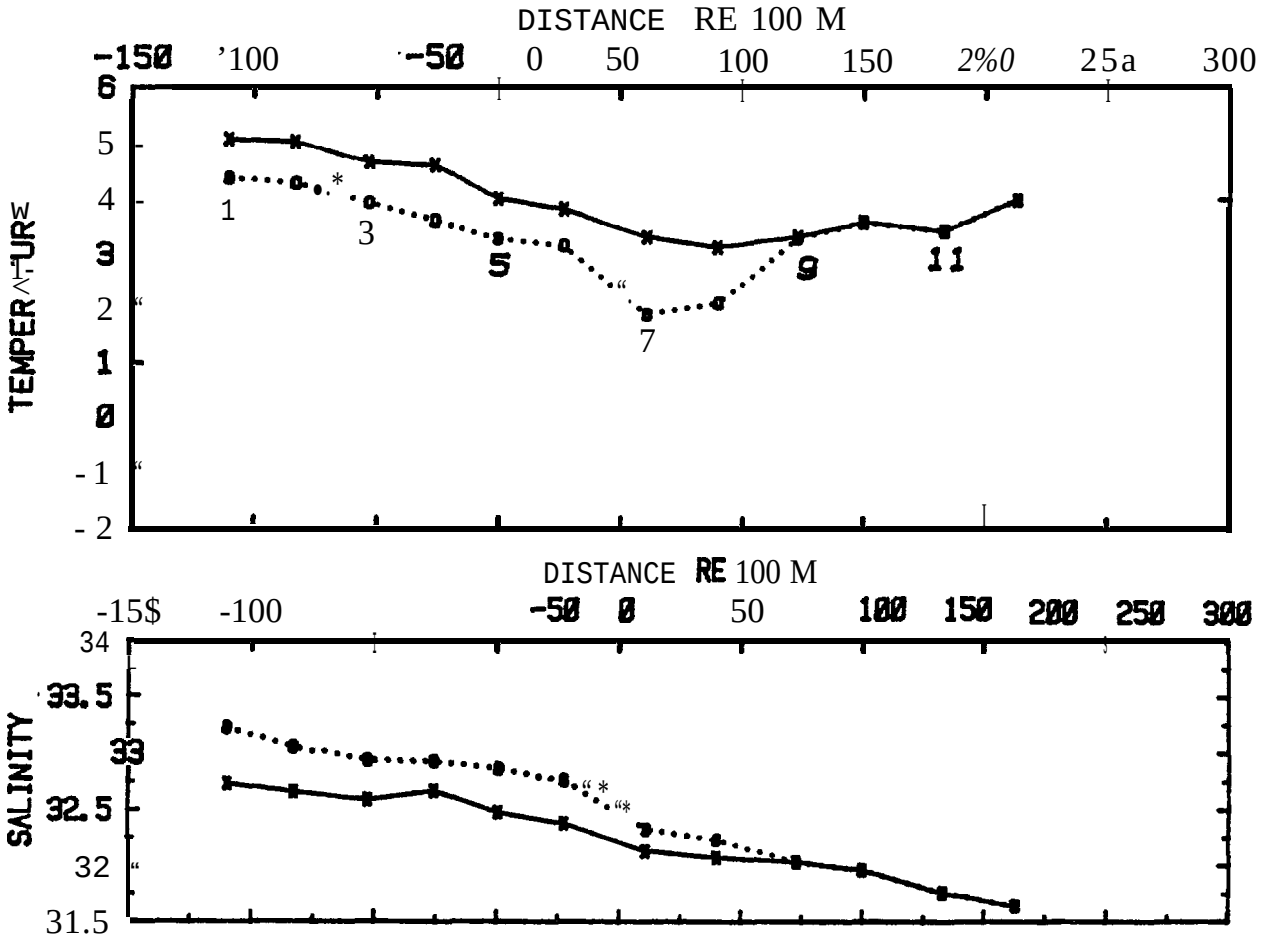

Figure 5.1. F-80A. Surface (x-x) and lower (0···0) layer temperature (°C) and salinity (ppt) versus distance (km) relative to the 100 m isobath along the Section.

- F-80B. This section lies about 300 km northwest of the F-80A section described above (Figure 2.1). Figures 5.4 through 5.6 show the upper and lower layer temperature (°C) and salinity (ppt) versus distance (km), the vertical stratification, and T-S characteristics along the section. Though the temperatures along this section tended to be lower than along F-80A, the horizontal gradients and the shape of the T-S correlations were similar. Both upper and lower layer temperatures decreased (-7 x 10^{-3}°C/km and -9 x 10^{-3}°C/km respectively) from near the shelf edge northward to Station 20. From Station 20 northward temperature increased in both the upper (+5 x 10^{-3}°C/km) and lower (+9 x 10^{-3}°C/km) layers. Salinity decreased monotonically (-3 x 10^{-3}

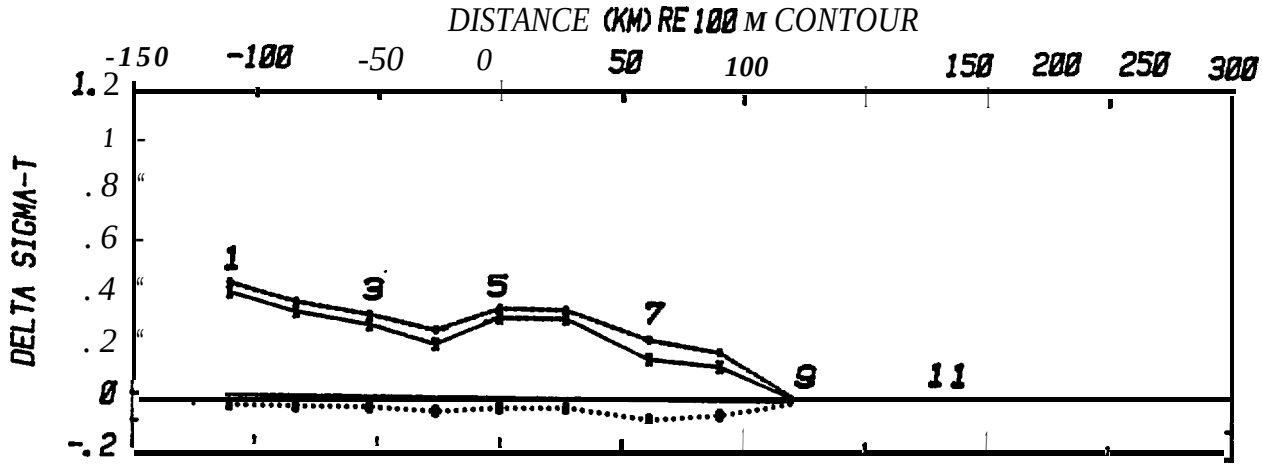

Figure 5.2. F-80A. Vertical stratification versus distance (km) relative to the 100 m isobath. The individual components, $\alpha\Delta T$ (0···0) and $\beta\Delta S$ (x–x) and the total stratification, $\beta\Delta S - \alpha\Delta T$ are plotted in units of Sigma-T.

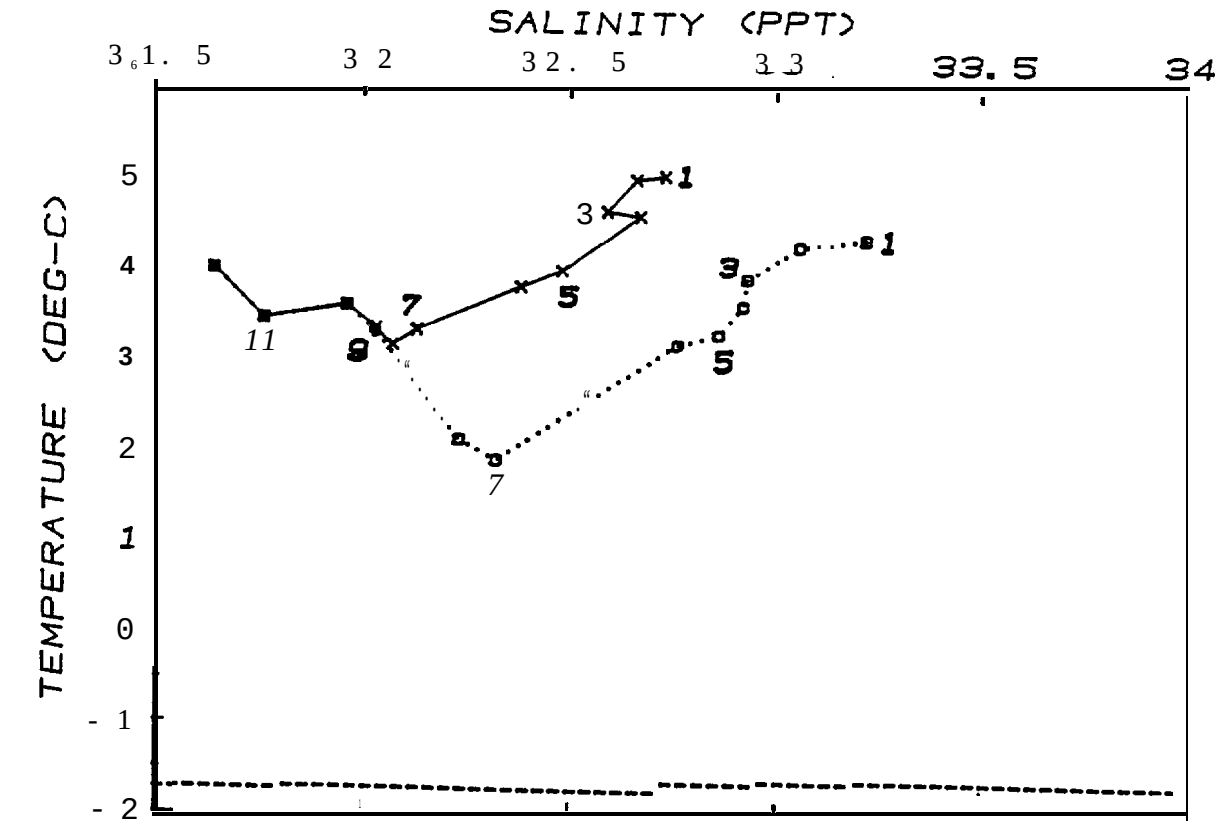

Figure 5.3. F-80A. Temperature-salinity characteristics proceeding from deepwater northward for upper (x-x) and lower (0-●-*0) layers.

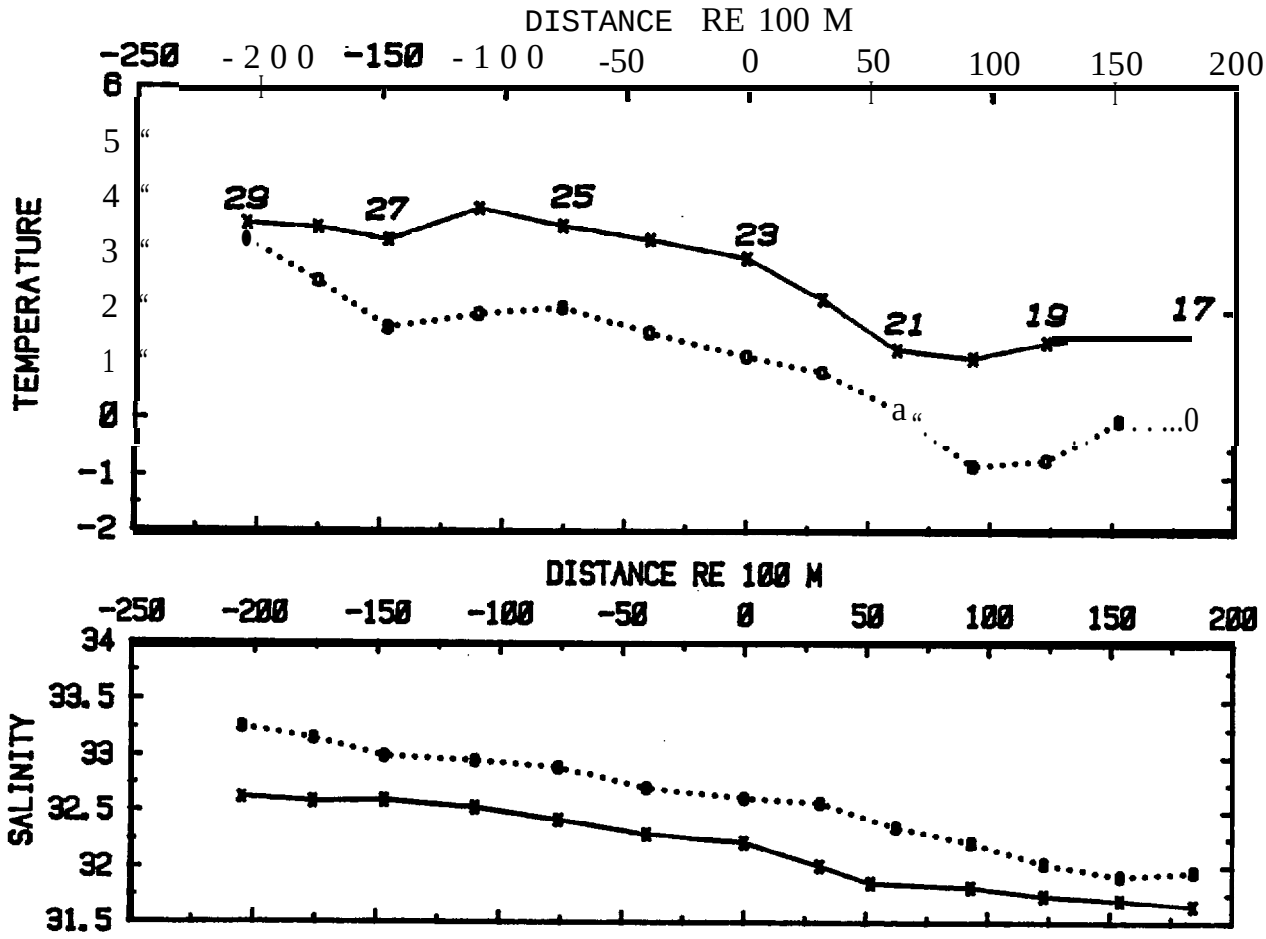

Figure 5.4. F-80B. Surface (x-x) and lower (O-●O) layer temperature (°C) and salinity (ppt) versus distance (km) relative to the 100 m isobath along the Section.

ppt/km in both layers) northward along the section. The slopes of the T-S correlations were similar to those along Section F-80A; dT/dS = +2.7°C/ppt (upper layer) and +2.9°C/ppt (lower layer) south of the temperature minimum (Station "20) and dT/dS = -3.0°C/ppt north of the temperature minimum.

Vertical stratification (Figure 5.5) was two-layer throughout the section. Stratification decreased from 0.5 sigma-t units near the shelf edge to about 0.3 sigma-t units at the north end of the section. Both the vertical temperature and salinity gradients were stabilizing.

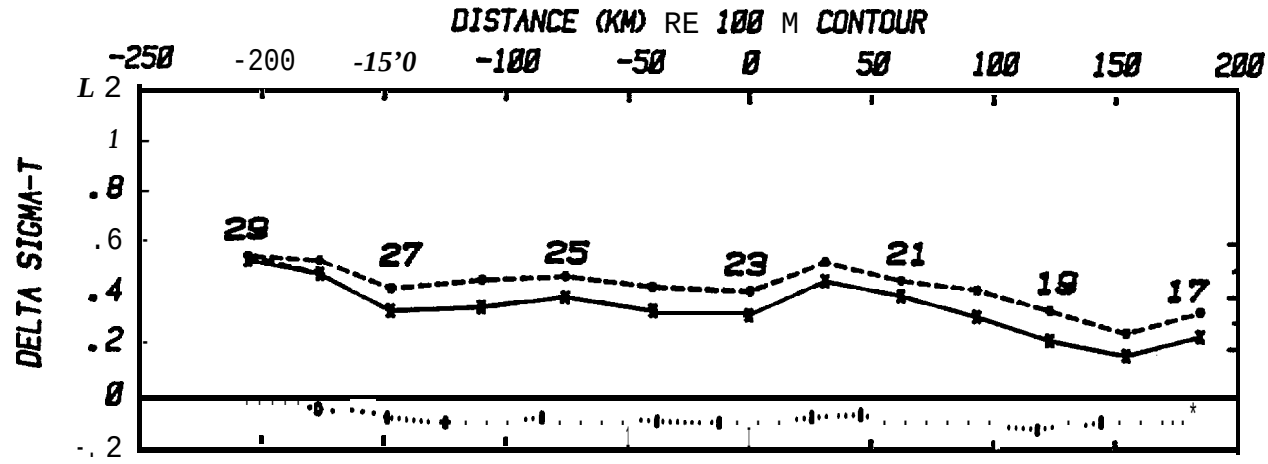

Figure 5.5. F-80B. Vertical stratification versus distance (km) relative to the 100 m isobath. The individual components, αΔT (0-·-0) and βΔS (x-x) and the total stratification, βΔS-αΔT are plotted in units of Sigma-T.

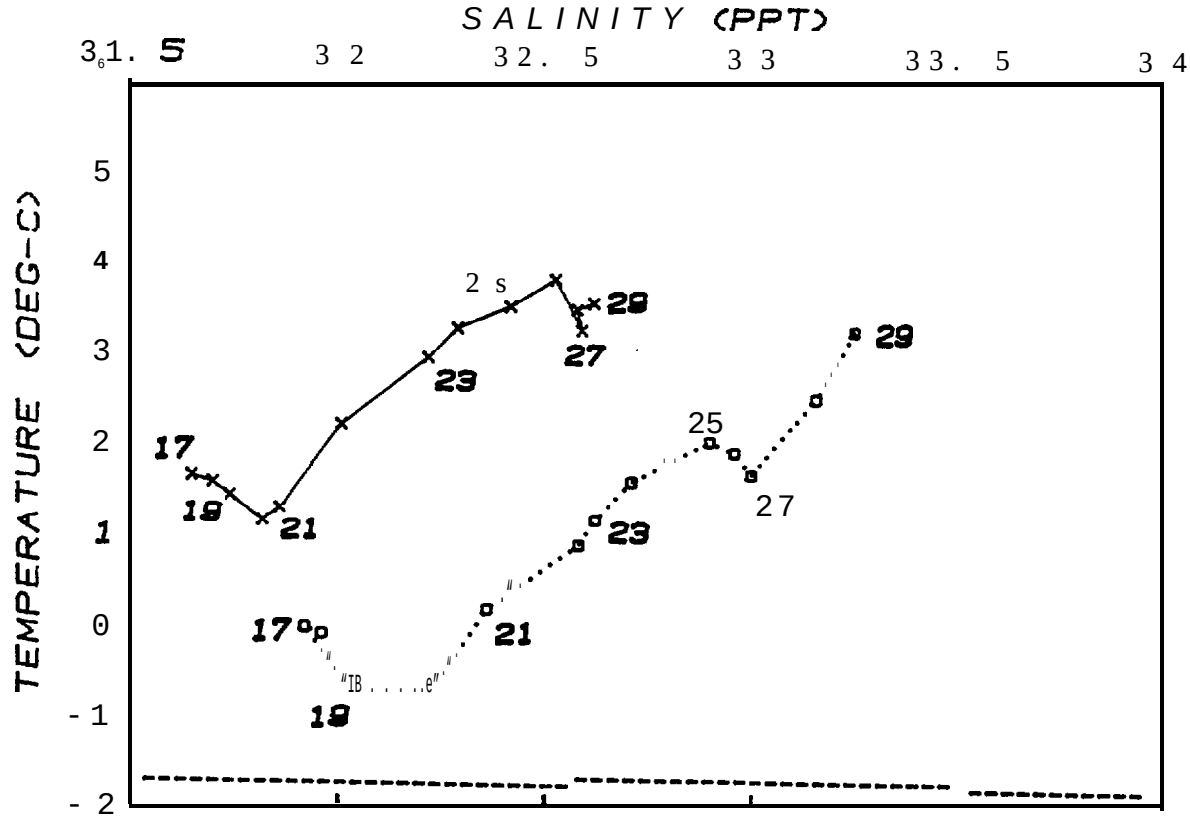

Figure 5.6. F-80B. Temperature-salinity characteristics proceeding from deepwater northward for upper (x-x) and lower (OO ..0) layers.

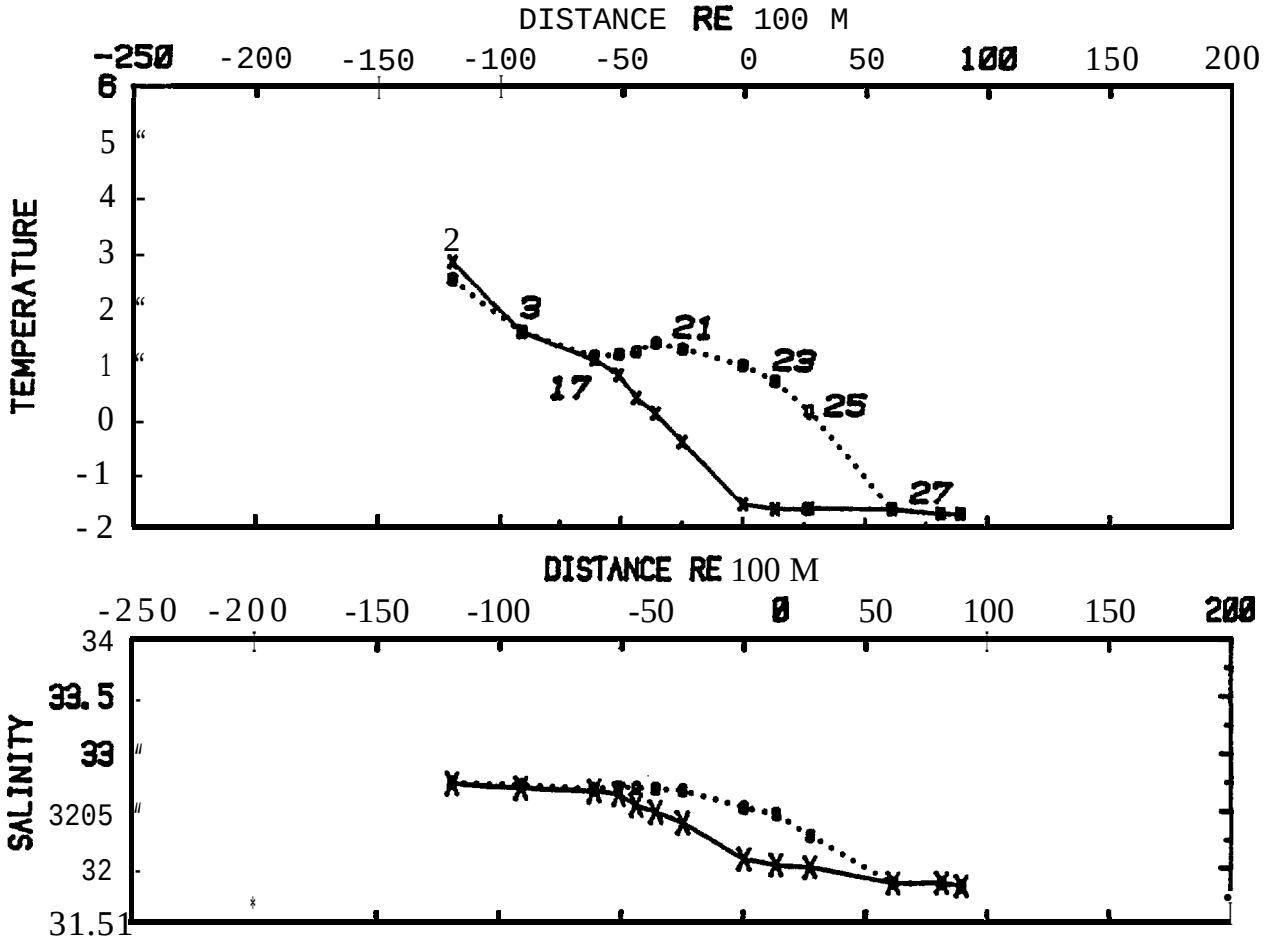

Figure 5.7. W-81. Surface (x-x) and lower (0···0) layer temperature (°C) and salinity (ppt) versus distance (km) relative to the 100 m isobath along the Section.

- W-81. This section essentially repeats the F-80A section (Figure 2.1). Proceeding north from Station 2 toward the ice edge (Figure 5.7) upper 1 ayer temperature decreased (-4.4 x 10^{-2}°C/km) to near the freezing point as salinity also decreased (-1 x 10^{-2} ppt/km). Lower layer temperature and salinity decreased to the north but over a greater horizontal distance (1.0 x 10^{-3}°C/km and 4 x 10^{-3} ppt/km respectively). Vertical stratification was essentially zero at the seaward and northward end of the section (Figure 5.8) with a maximum of 0.2 sigma-t units occurring near the 100 m isobath. The along-section T-S correlations (Figure 5.9) are positive (dT/dS = +4.4°C/ppt (upper layer) and +2.6°C/ppt (lower layer).

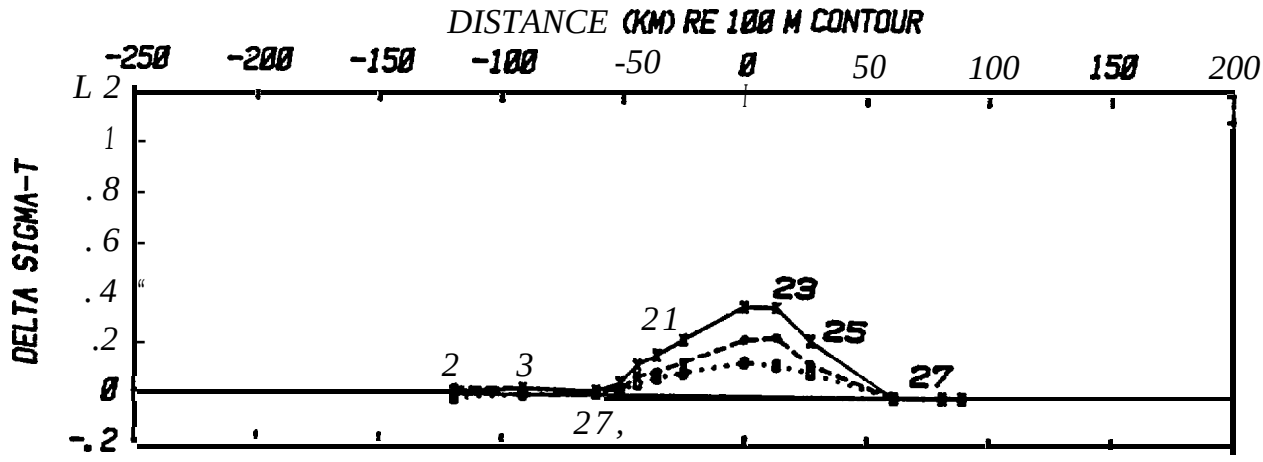

Figure 5.8. W-81. Vertical stratification versus distance (km) relative to the 100 m isobath. The individual components, $\alpha\Delta T$ (0···0) and $\beta\Delta S$ (x–x) and the total stratification, $\beta\Delta S-\alpha\Delta T$ are plotted in units of Sigma-T.

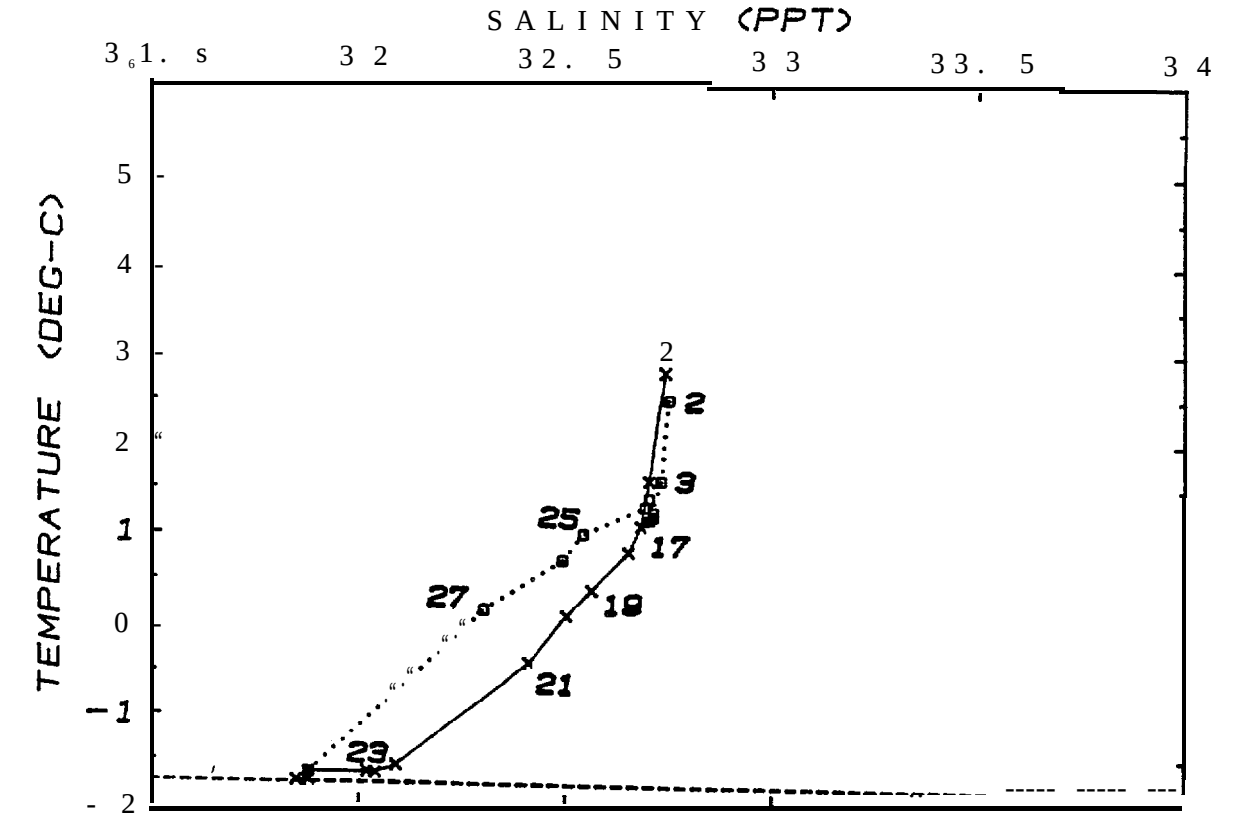

Figure 5.9. W-81. Temperature-salinity characteristics proceeding from deepwater northward for upper (x-x) and lower (0···0) layers.

5.2 Regional Characteristics of the Wintertime Hydrographic Structure

Three of the CTD sections discussed above, W-80A, W-81 and W-80B, crossed the Bering Sea MIZ at about 250 km intervals from the southeastern shelf (W-80A) to the central shelf (W-80B). Noting that the middle section (W-81) is from a different year, these sections will be discussed as a group to provide a regional description of the temperature, salinity and density structure of the MIZ.

Figure 5.10 shows the location of the three sections and plots the approximate position of the ice edge based on the Navy-NOAA Joint Ice Center analyses for 26 Feb and 4 Mar 1980, coincident with Section W-80A, 25 Mar and 1 Apr 1980, coincident with Section W-80B, and 3 and 10 Mar 1981 corresponding to Section W-81. Over the southeastern shelf, east of 172°W, the ice edge during these periods was positioned over rather shallow water, 50-100 m, and showed a significant amount of variability (~200 km) in the north-south direction. West of 172°W, over the central and eastern shelf, the ice edge positions for these periods tended to be nearly coincident. West of 172°W the ice edge occurred over deeper water and appeared to be nearly aligned with the 200 m isobath.

Wintertime hydrographic structure in the MIZ based on the 1980-81 data generally could be characterized as two-layer (Figures 4.1a and b, 4.7a and b and Muench, 1981). The upper layer was on the order of 50 m thick and the lower layer was usually 25-75 m in vertical extent. The temperature and salinity of the upper and lower layers along the shelf is plotted in Figures 5.11a and b and 5.12a and b. The heavy line segments indicate where the contoured values occur along the sections. Dashed lines are used to connect equal values along the shelf but should not be construed as contours because of the wide spacing (~250 km) of the CTD lines. The temperature of the upper layer changed from cool (<-1.5°C) to relatively warm (>0°C) over a distance of about 50 km. This relatively sharp horizontal temperature gradient was coincident with a salinity change (Figure 5. 11b) of 0.25 ppt or greater over the same distance. This temperature and salinity front occurred roughly coincident with the ice edge (Figure 5.10) and thus, proceeding westward, tended to be positioned over progressively deeper water. North of the -1.7°C isoline in Figure 5.11a,

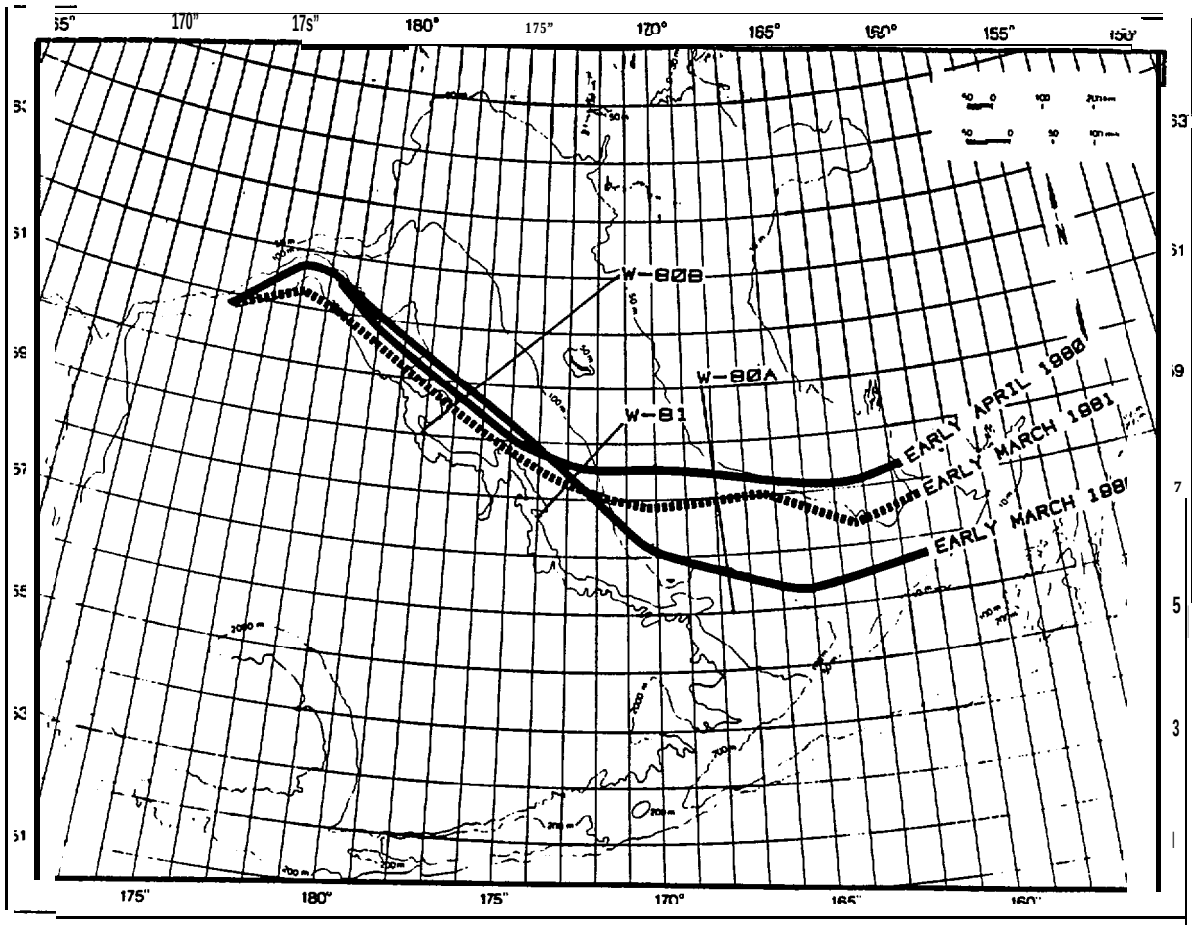

Figure 5.10. Approximate location of the ice edge based on NAVY-NOAA Joint Ice Center analyses for (1) Early March 1980 (26 Feb and 4 Mar; Section W-80A), (2) Early April 1980 (25 Mar and 1 Apr; Section W-80B), and (3) Early March 1981 (3 Mar and 10 Mar; Section W-81).

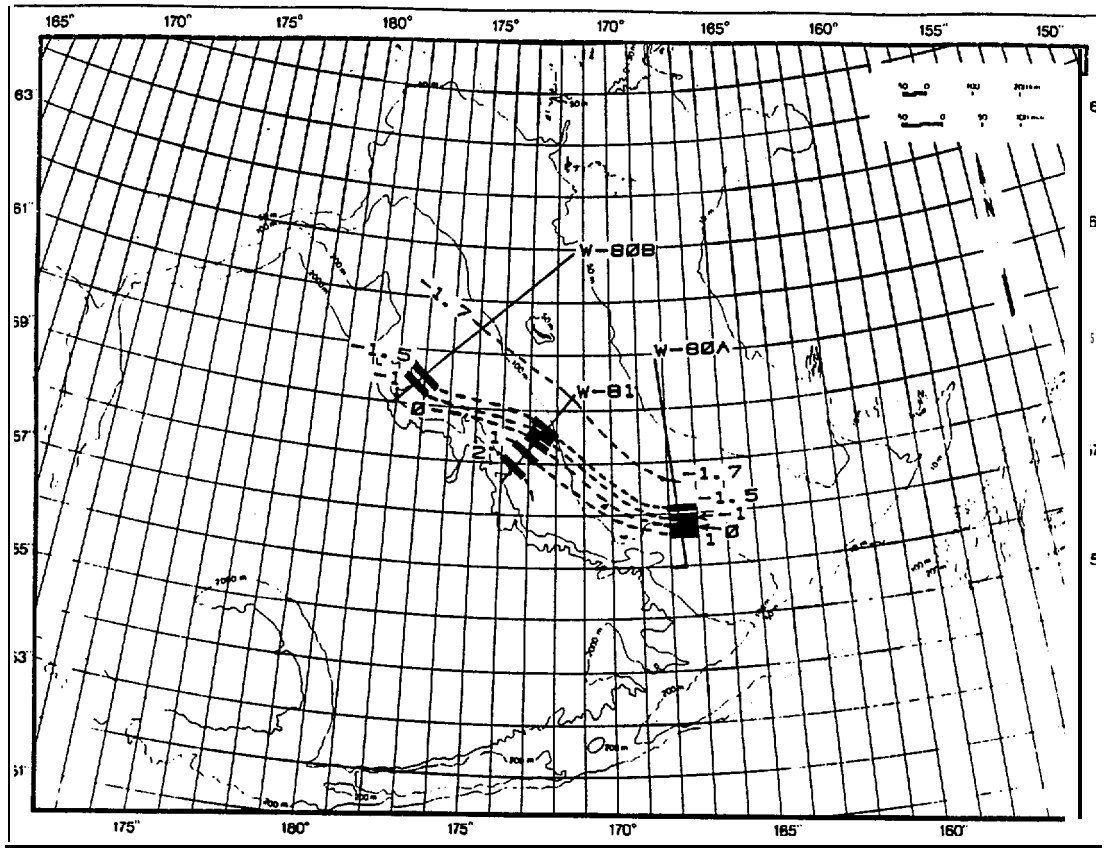

Figure 5.11a. Upper 1 ayer temperature (oC)

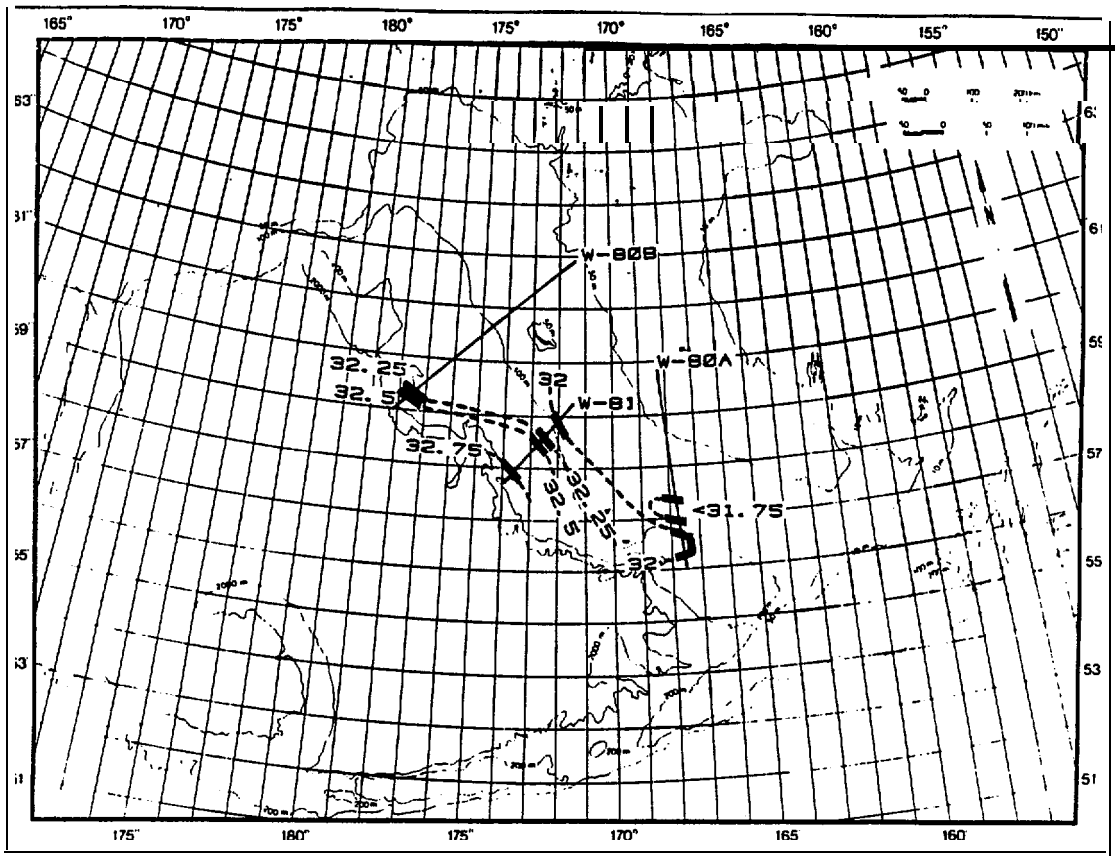

Figure 5.11b. Upper layer salinity (o/oo)

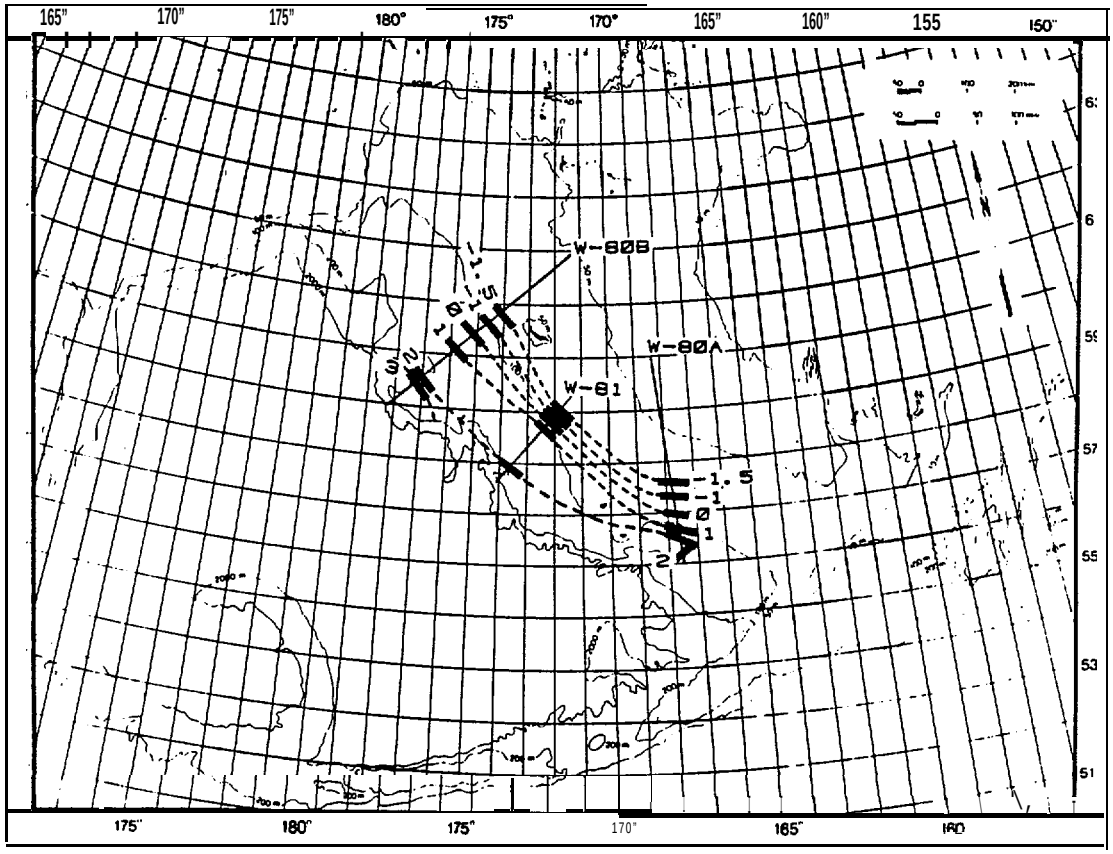

Figure 5.12a. Lower layer temperature (oC)

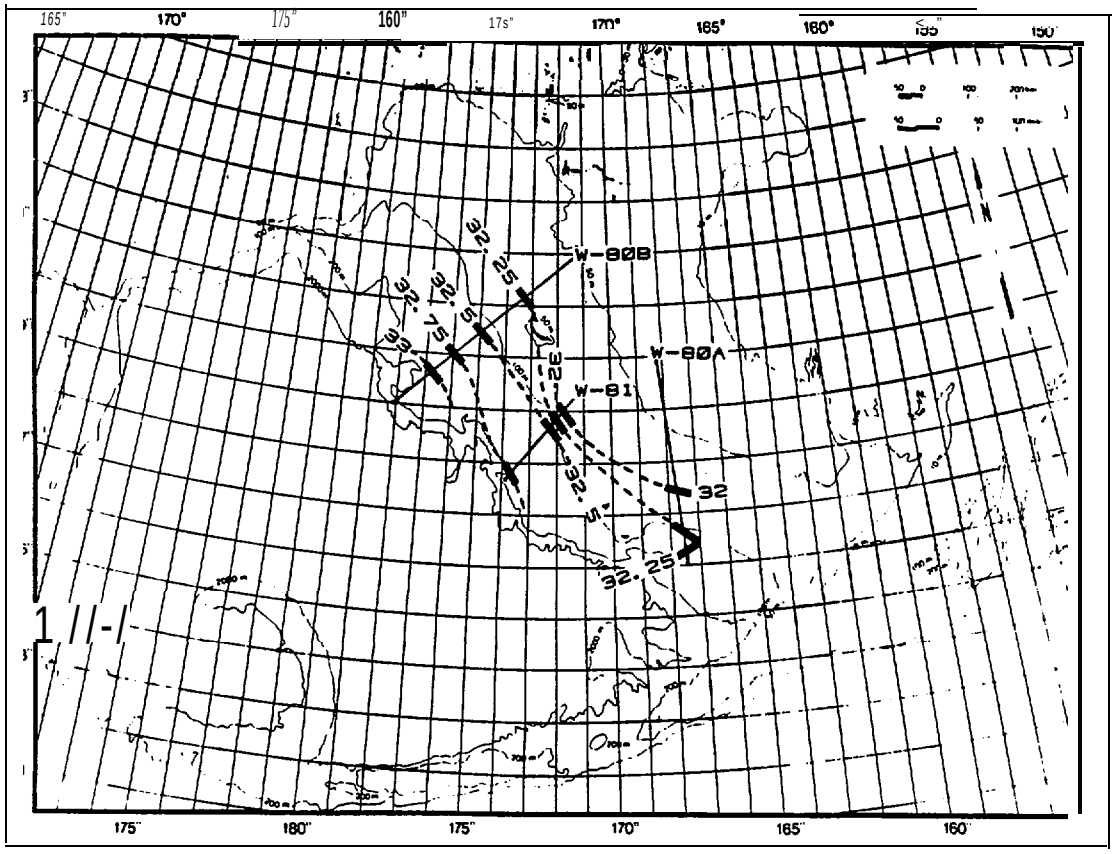

Figure **5.12b.** Lower layer salinity (o/oo)

surface layer temperatures were essentially at the freezing point for the associated salinity. South of the -1.7°C isoline to the ice edge, a distance of 50 to 200 km, upper layer temperatures were significantly elevated (>0.10°C) above their freezing point.

Throughout the MIZ lower layer temperatures and salinities (Figure 5.12a and b) were greater than those of the upper layer. Lower layer temperature and salinity for the 1980 sections changed more regularly in the north-south direction and did not show a sharp transition or front. Section W-81 however, did have a high gradient region in the lower layer for both temperature and salinity at about the 100 m contour.

Though temperature increased with depth, the effect on density of the increased salinity resulted in a stably stratified water column throughout the MIZ. The stability, expressed as the difference in sigma-t between the lower and upper layer is plotted in Figure 5.13. North of about the 75m contour, the water column is essentially vertically homogeneous. Stratification increases south toward the ice edge, reaching a maximum (Δsigma-t $\sim$.3 in W-80A, W-81 and Δsigma-T = $\sim$.8 in W-80B) near the ice margin.

The dynamic height of the surface (O db) relative to 50 db is plotted in Figure 5.14. The strongest baroclinic current shear (closely spaced isolines) occurred near the ice edge over the central shelf (W-81 and W-80B). Computed baroclinic currents in this region were on the order of 3-4 cm/sec. North of the ice margin baroclinic currents were weak (<1 cm/sec on the average) and possibly evidenced some eddy-like motions (for example in the north part of Section W-80B).

5.3 Seasonal Changes in Heat and Salt

Two pairs of CTD sections provide a measure of winter to fall and fall to winter changes in heat and salt content within the Bering Sea MIZ. These pairs are W-80B and F-80B (April 1980 and November 1980, separated by 227 days) which crossed the central shelf northwest of St. Matthew Island and F-80A and W-81 (November 1980 and March 1981, separated by 112 days) which crossed the central shelf southeast of St. Matthew Island.

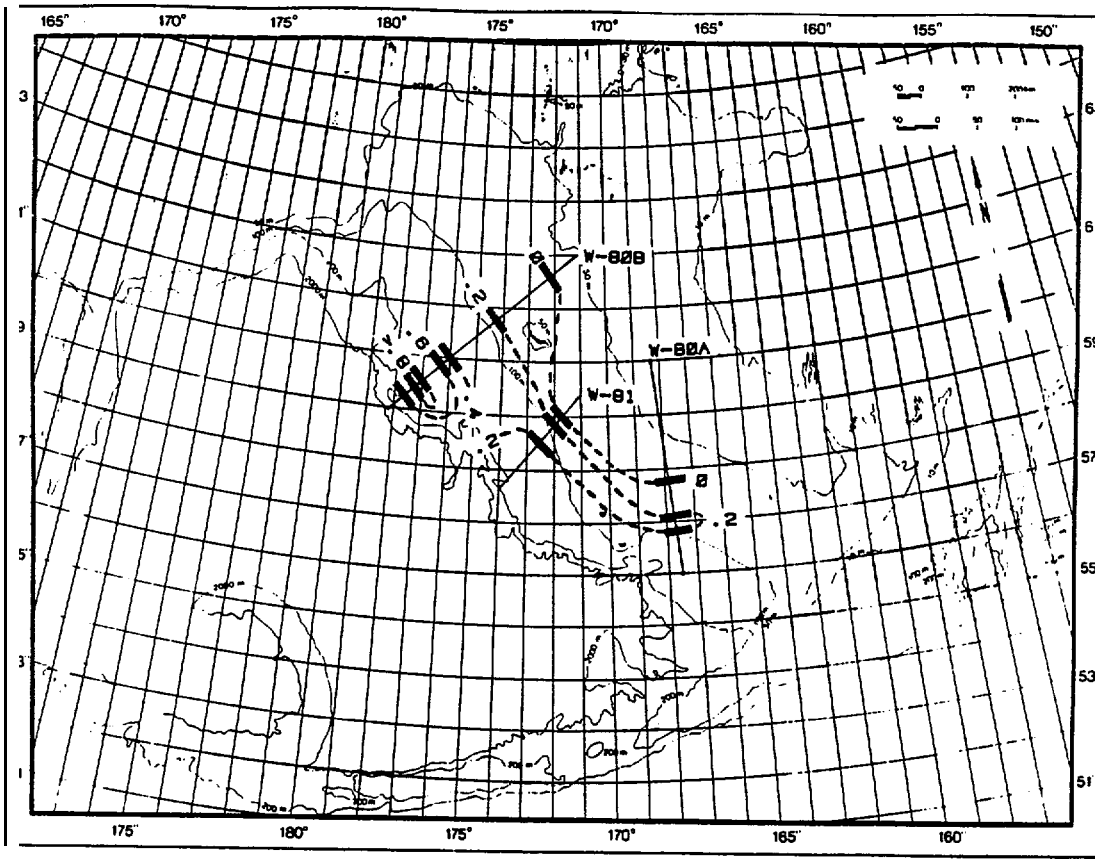

Figure 5.13. Vertical stratification, sigma-t difference between lower and upper layers.

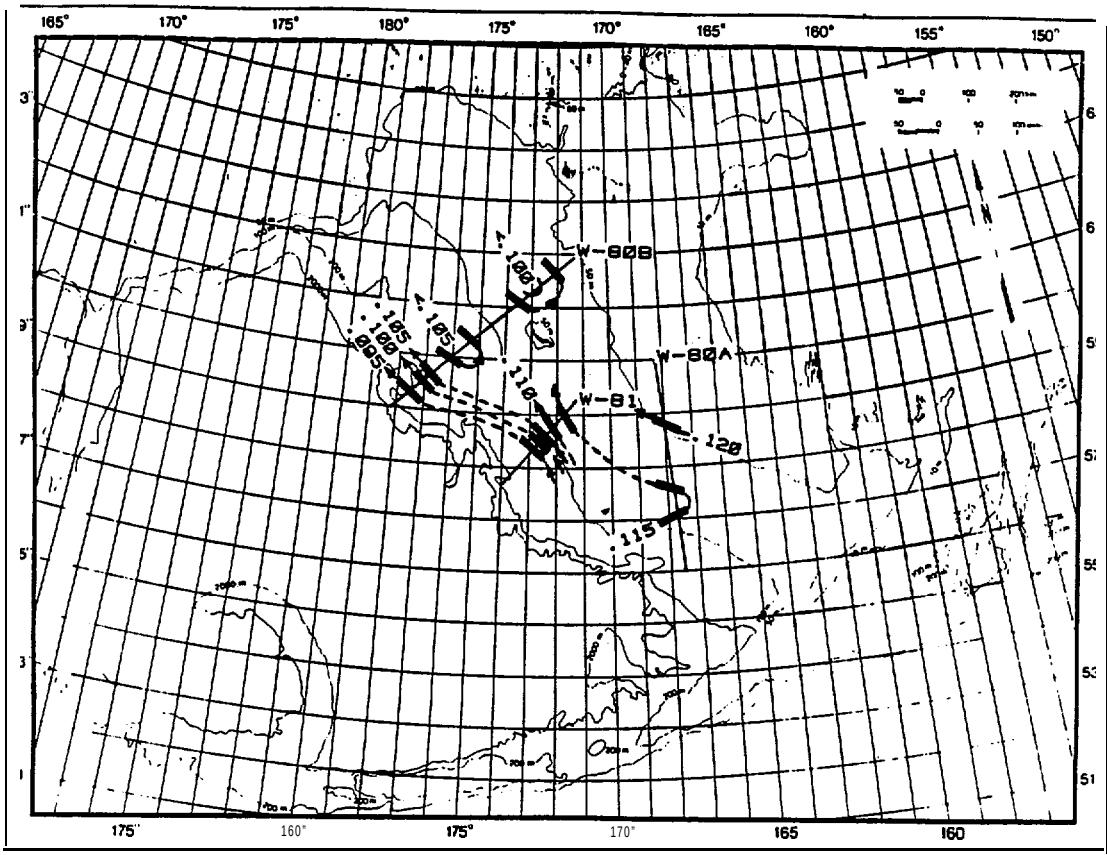

Figure 5.14. Dynamic height (dyn-m) relative to 50 db

Figures 5.15a and b plot the lines of stations which make up the W-80B — F-80B and F-80A — W-81 sections and indicate the position of the 100 m isobath. For this comparison these station lines were divided into 25 km intervals. A single hydrographic station within an interval was assumed to be representative of conditions within that segment; two or more stations within an interval were averaged to provide temperature and salinity profiles typical of the interval. The station lines making up each comparison were matched at the 100 m isobath for the purpose of the following calculations.

For each 25 km interval the change in heat content between fall and winter was calculated as:

$$\Delta H_{F\rightarrow W} = \rho C_p \int_0^D (T_W - T_F)\, dz \ , \qquad (2)$$

where $\Delta H_{F\rightarrow W}$ [cal] is the change heat content of a column of water 1 cm^2 in area of height D[cm] between winter 1980 and the subsequent fall 1980 (W-80B → F-80B) or winter 1981 as the previous fall (W-81 ← F-80A)

ρ[gm/cm^3] is the density, ≅1.03 gm/cm^3

C_p[cal/gm-^oC] is the specific heat, ≅0.94 cal/gm-^oC

D[cm] is depth of the water, and

T_W, T_F are the Winter and Fall temperature [^oC] profiles as a function of depth [z].

The above computation was carried out for each 25 km interval along both pairs of sections. Separate calculations were made for the mixed surface layer, for

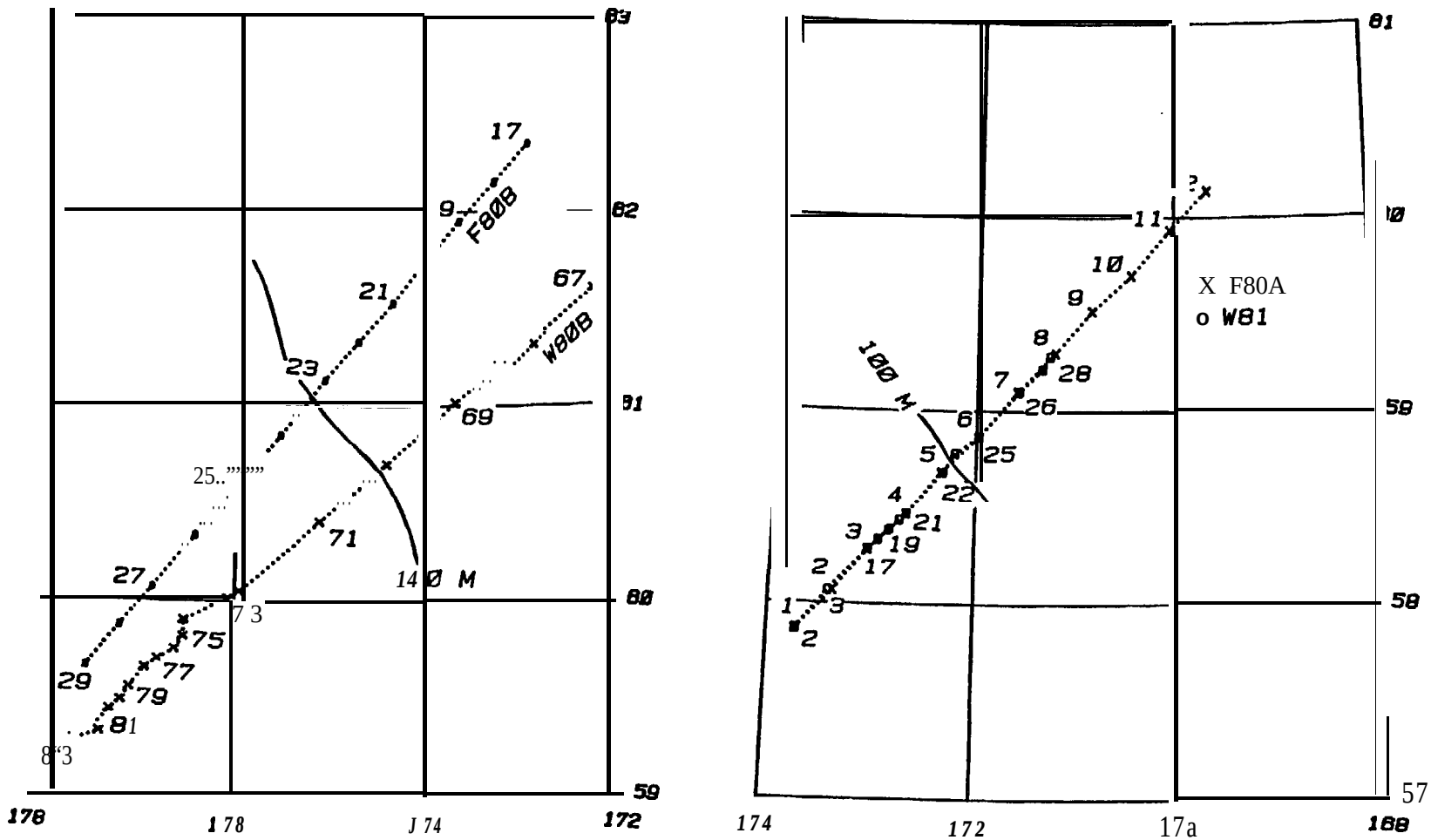

Figure 5.15. Positions of CTD stations for (a) F-80A and W-81 and (b) F-80B and W-80B sections.

water column from the base of the surface layer to the ocean bottom and for their sum, the total change in heat content. The results are plotted in Figures 5.16a and b.

Similarly, the change in salt content was computed for the same cases by:

$$\Delta S_{F\to W} = \rho \cdot 10^{-3} \int_0^D (S_W - S_F)\, dz \qquad (3)$$

where $\Delta S_{F\to W}$ [gin] is the change in salt content of a column of water 1 cm2 in area of height D[cm].

ρ[gm/cm^3] is the density, ≅1.03 gm/cm^3,

D[cm] is the depth of the water, and

S_F , S_W are the Fall and Winter salinity (ppt) profiles as a function of depth [z].

The equivalent thickness of ice melting ($\Delta S<0$) or freezing ($\Delta S>0$) required to produce the change in salt content was estimated by:

$$i = 10^3 \Delta S/[.9(\bar{S}-Si)] \qquad (4)$$

where i is the thickness of ice melt (or freezing)

ΔS [gm] is the change in salt content over the appropriate layer

Si (g/kg) is the salinity of the ice [≅7 g/kg]

$\bar{S}$ (g/kg) is the average initial salinity of the layer, and

.9 is the density of sea ice [gm/cm^3] .

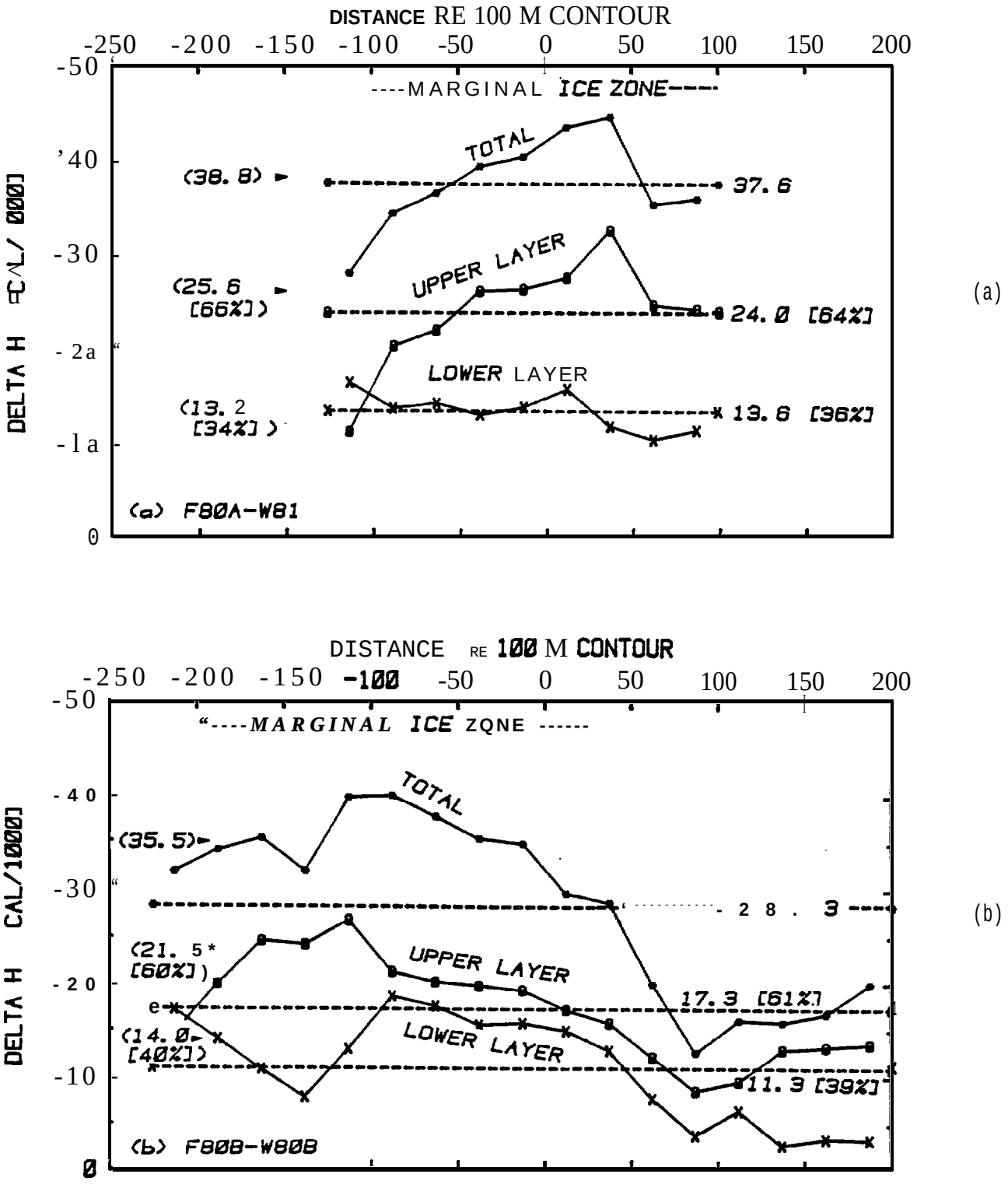

Figure 5.16. Change in heat content, $\Delta H[Cal/cm^2]$, for 25 km intervals; (a) F-80A - W-81 and (b) F-80B - W-80B. Along section averages are shown for the total section length (dashed lines) and for the MIZ (averages shown in parentheses).

The change in salt content [gin] and the equivalent dilution/concentration by ice melting/freezing expressed in meters are plotted in Figures 5.17 and 5.18 a and b.

The F-80A–W-81 comparison, a 225 km line approximately centered on the 100 m isobath, is limited by the length of the W-81 CTD section, obtained when the wind pushed the ice northward. Except for the southern most 25 km segment which appears to be influenced by the oceanic domain this section can be considered to have crossed the MIZ. The total change in heat content averaged over the MIZ portion of this section was 3.88 x 10^4 cal/cm^2 during the November 80 to March 81 (112 day) period. Of this total change in heat content, 2.55 x 10^4 cal/cm^2 [66%] occurred in the upper layer and 1.36 x 10^4 cal/cm^2 [34%] were extracted from the lower layer extending from the base of the surface layer to the bottom. The heat loss was a maximum in the 25-50 km interval north of the 100 m isobath and decreased to the north and south (Figure 5.16a). The change in salt content averaged along the MIZ portion of this section (Figure 5.17a) was 2.3 g/cm^2 of which 1.3 gm/cm^2 [56%] was due to freshening of the surface layer in the winter and 1.0 gm/cm^2 [44%] was a result of lower layer freshening. Except for the seaward 25 km interval, which might have been influenced by oceanic domain waters the salt deficit was a maximum just north of the 100 m isobath, coincident with the maximum in the heat loss (Figure 5.16a). The salt deficit (Figure 5.17a) is converted to equivalent meters of ice melt/freezing in Figure 5.18a. The maximum salt deficit, at 25-50 km north of the 100 m isobath, is equivalent to the melting' of 1.6 m of ice per cm^2.

The F-80B — W-80B comparison covers a line of nearly 400 km across the MIZ onto the Bering shelf. North of the interval which lies 25-50 km north of the 100 m contour, the salt deficit is positive (Figure 5.17b) suggestive of freezing conditions during the winter of 1980. Thus the MIZ will be considered to be the region from 200 km seaward of the 100 m depth contour to 25 km shelfward of the 100 m isobath. This also corresponds to that region where the wintertime (W-80B) upper (and lower) layer temperatures were significantly above (>+0.10°C) freezing (Figure 4.11). The total change in heat content from fall 1980 to winter 1981 was 3.55 x 10^4 cal/cm^2 averaged over the section with 2.15 x 10^4 cal/cm^2 [60%] of the change in the upper layer

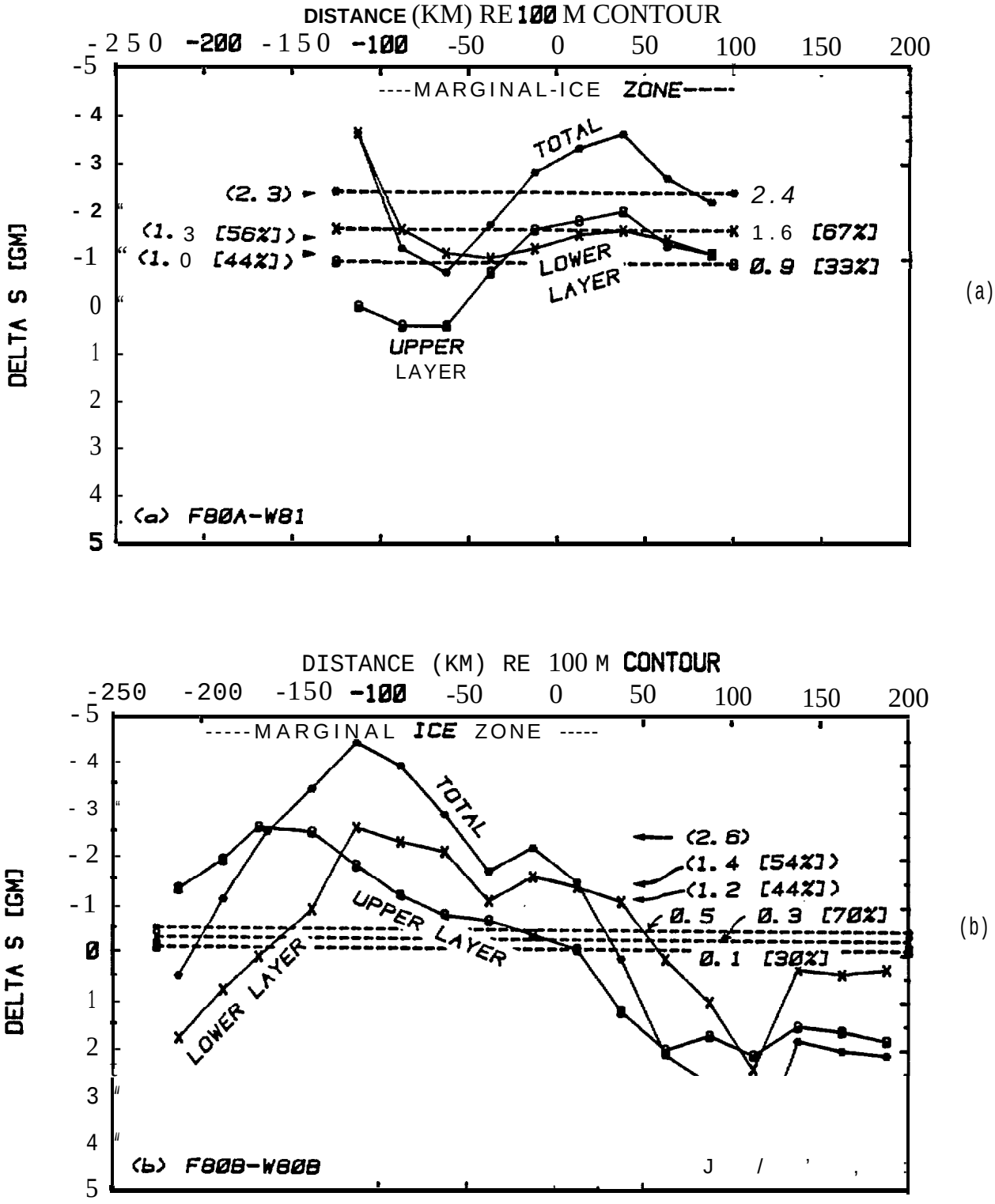

Figure 5.17. Change in salt content, $\Delta S[gm/cm^2]$, for 25 km intervals. (a) F-80A – W-81 and (b) F-80B – W-80B. Along section averages are shown for the total section length (dashed lines) and for the MIZ (averages shown in parentheses).

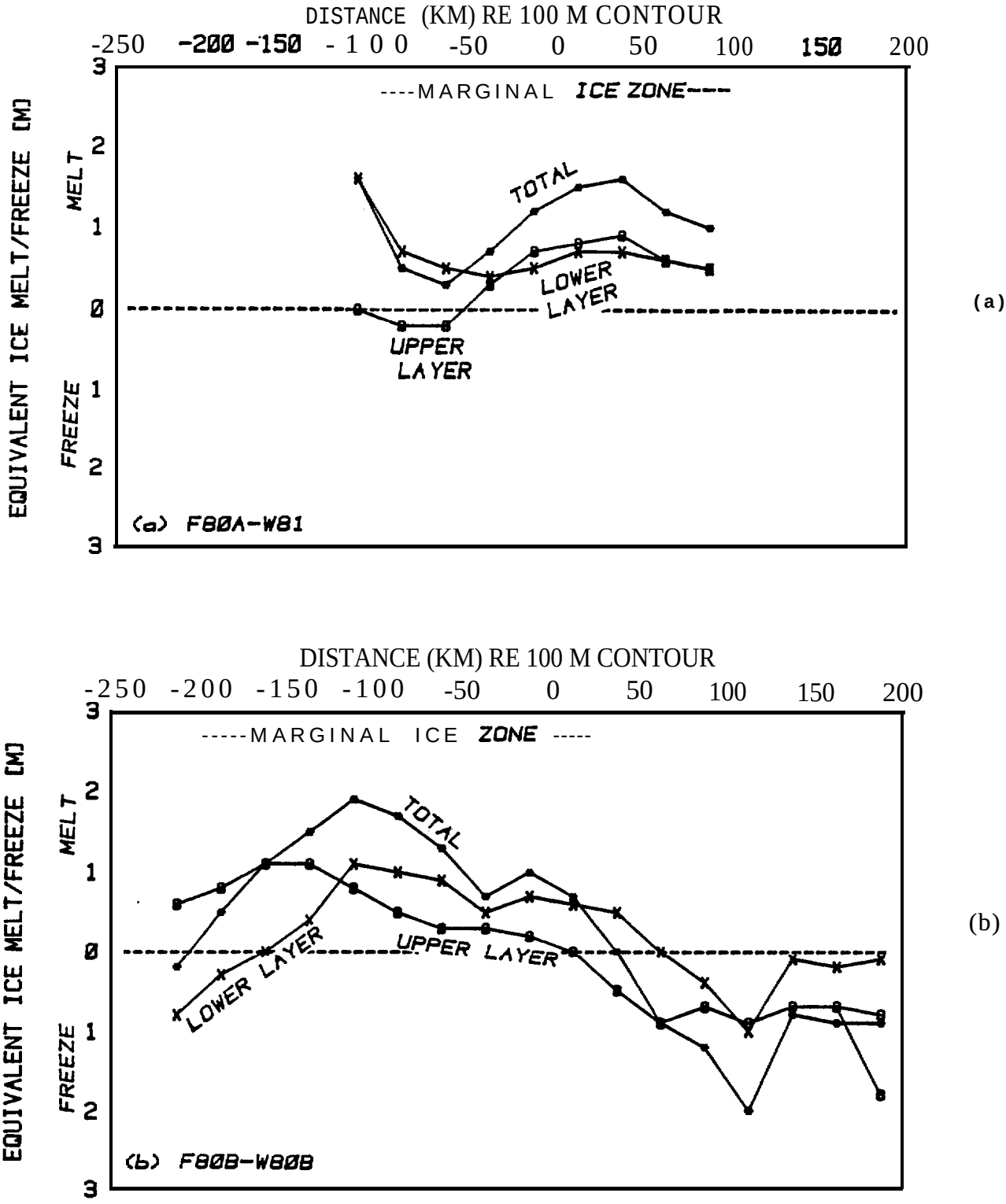

Figure 5.18. The thickness of ice at 7°/00 in meters which must melt (-) or freeze (+) to produce the observed change in salt content;; (a) F-80A – W-81 and (b) F-80B – W-80B.

and a 1.40 x 10^4 cal/cm^2 [40%] of the change in the water column extending from the base of the upper layer to the bottom. The maximum heat content change occurred about 100 km seaward of the 100 m isobath. The average salt deficit in winter was 2.6 gm/cm^2 with 1.4 gm/cm^2 [54%] in the upper layer and 1.2 gm [46%] from below the pycnocline. The maximum in wintertime salt deficit (Figure 5.17b) occurred coincident with the maximum in the heat loss at about 100 km seaward of the 100 m isobath. The maximum total salt deficit was equivalent to the melting of 1.9 m of ice per cm^2 area.

Table 5.1 summarizes the average changes in heat and salt content across the MIZ for the two comparisons. The total change in heat content was about the same (within 10%) for both comparisons. Just over 60% of the total change in heat content was a result of heat extracted from the upper layer and the remainder (a little under 40%) occurred at depths below the pycnocline. Similarly, the change in total salt content was within 15% for the two comparisons with just over 50% of the salt deficit attributed to the upper layer and somewhat less than 50% due to freshening of the waters below the pycnocline.

A simple box model of heat and salt exchange in the MIZ which neglects advection is sketched in Figure 5.19. During the fall to winter period heat will be lost: (1) from the upper layer through surface exchange and (2) from the lower layer by a two step process of first mixing of the warm lower layer waters into the upper layer and then exchange through the surface. The melting of ice in the MIZ will (3) extract heat from the upper layer and (4) from the lower layer in the presence of vertical mixing. Accompanying the heat loss associated with ice melt will be a reduction in the salt content of the (5) upper and (6) lower layer due to the addition of fresh water. For this simple model the change in heat and salt content (expressed as equivalent ice melt) from fall to winter can be expressed as:

$$\Delta H_{F \to W} = \Delta H_0 + \rho L i \qquad (5)$$

where $\Delta H_{F \to W}$ total change in heat content [cal] per cm^2 area

Table 5.1. Summary of Changes in Heat and Salt Content from Fall to Winter Averaged Across the MIZ Portion of the Sections

		F80A-W81	F80B-W80B
Change in Heat Content [Cal/cm^2]	Total	3.88x10' (100%)	3. 55X104 (100%)
	Upper Layer	2. 56x10^4 (66%)	2. 15x10^4 (60%)
	Lower Layer	1.32x104 (34%)	1.40x10^4 (4o%)
Change in Salt Content [gm/cm^{2}1 (Equivalent Thickness of Ice Melting)	Total	2.3 (loo%) (1.00 m)	2.6 (100%) (1.10 m)
	Upper Layer	1.0 (44%) (0.48 m)	1.4 (54%) (0.57 m)
	Lower Layer	1.3 (56%) (0.52 m)	1.2 (46%) (0.53 m)

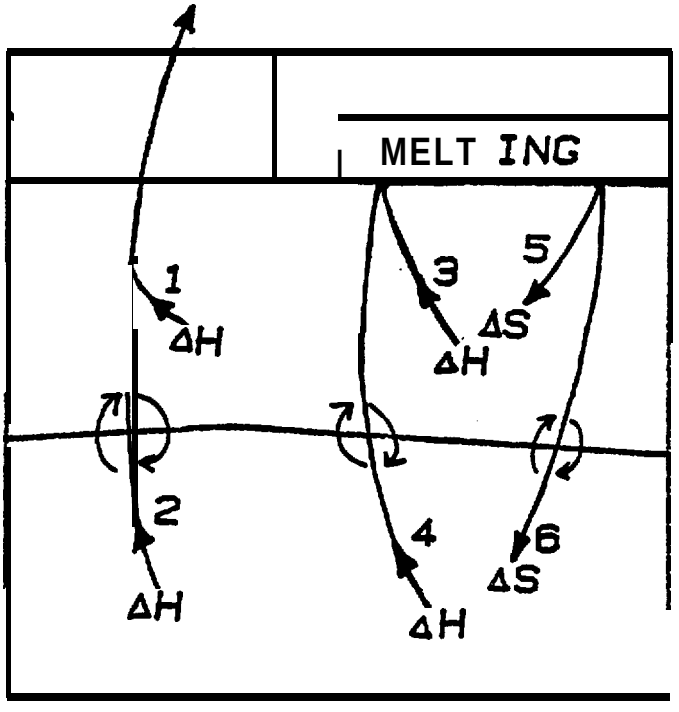

Figure 5.19. Schematic of changes in heat and salt content due to surface exchange and ice melting. Advective effects are neglected.

ΔH_o change in heat content due to surface exchange [cal] per cm^2 area

ρLi change in heat content due to ice melting [cal]; ρ = density of ice [g/cm^3]; L = latent heat of fusion for sea ice [cal/gm]; i = ice thickness [cm] per cm^2 area melting.

The latent heat of fusion of sea ice, L, which is the number of calories necessary to melt one gram of sea ice, is a variable function of the temperature and salinity of the ice (cf. Zubov, 1943, Table 40). For example in the rather narrow temperature range of -1 to -20C and salinity range of 6 to 8 ppt, L varies from 47 to 68 cal/gm. Choosing L = 60 cal/gm and using the values from Table 5.1, estimates for the terms in expression (5) are shown in Table 5.2.

Based on the average changes in heat and salt content from fall to winter and the assumptions above it appears that of the total heat loss, about 85% is due to surface exchange (with about 2/3 of this heat loss from the upper layer and 1/3 from the lower layer). About 15% of the total heat loss can be associated with the process of the melting of sea ice in the MIZ.

As it appears that the changes in heat content are, at least visually (Figures 5.17, 5.18 and 5. 19), somewhat correlated with the changes in salt content along the sections, it may be possible to estimate the terms in equation (5) by a linear regression using the individual data pairs for each 25 km interval. The regression, $y = a + bx$, was computed for each section on the data from the upper layer, lower layer and total water column with $y = \Delta H_{F \to W}$, $X = i$, and thus a estimates ΔH_0 and b estimates ρL. The results of the regression analyses are summarized in Table 5.3. With one exception (the F-80B — W-80B total case) the correlations between $\Delta H_{F \to W}$ and i for the upper layer and the total water column were significantly different from zero at the 5% confidence level. The correlations for the lower layer data were not significantly different from zero.

Table 5.2. Estimates of the Heat Balance Terms [Cal/cm²] in Equation (8) Based on the Averaged Data in Table 5.1

	$\Delta H_{F \to W}$	AH_0	ρL_i
Total	3.88×10^4	3.34×10^4	0.54×10^4
F80A-W81 Upper Layer	2.56×10^4	2.30×10^4	0.26×10^4
Lower Layer	1.32×10^4	1.04×10^4	0.28×10^4
Total	3.55×10^4	2.96×10^4	0.59×10^4
F80B-W80B Upper Layer	2.15×10^4	1.86×10^4	0.29×10^4
Lower Layer	1.40×10^4	1.11×10^4	0.29×10^4

Table 5.3. Summary of Parameters for Regression Analysis of AH Versus i (Equation 1) for the 25 km Intervals Across theMIZ

		F80A → W81	F80B → W80B	Combined F80A-W81 & F80B-W80B
Total	n	8	9	17
	r	0.72*	0.64	0.53*
	AH_0	3.28×10^4	3.03×10^4	3.23×10^4
	ρL	59.4	44.8	43.7
Upper Layer	n	8	9	17
	r	0.86*	0.82*	0.62*
	AH_0	2.13x10*	1.79×10^4	2.0X104
	PL	91.1	62.8	65.3
Lower Layer	n	8	9	17
	r	0.13	0.52	0.45
	AH_0	1.21×10^4	1.18×10^4	1.14×10^4
	PL	18.9	43.2	40.6

*Correlation coefficient significantly different from zero at the 5% significance level.

n = number of pairs

c = correlation coefficient

ΔH_0 = the intercept

PL = the slope of the regression line

The correlation between the temperature and salinity changes within each 25 km interval from fall to winter conditions are shown in Figure 5.20 for the upper mixed layer and for the lower layer, extending from the base of the upper layer to the bottom. Changes in upper layer temperatures ranged from -3.4°C to -5.5°C with salinity differences of -0.06 ppt to +0.52 ppt. There was a positive correlation between the temperature and salinity differences ($r = 0.75$, significantly different from 0 at the 1% significance level) with the slope, $\Delta T/\Delta S \cong 2.47$°C/ppt. Temperature and salinity differences for the lower layers ranged from -0.9°C to -4.0°C and -0.08 ppt to +0.54 ppt respectively. These AT-AS pairs were also positively correlated ($r = 0.81$, different from zero at the 1% confidence level) with a slope of $\Delta T/\Delta S \cong 4.7$°C/ppt. If the important processes for altering the surface layer temperature and salinity in the MIZ are ice melting and surface exchange then the temperature and salinity changes can be determined from:

$$\rho C_p a dT_W = \rho C_p a dT_F \quad AH_o - \quad \rho_i L i a \qquad (6)$$

[heat content, fall] [heat content, winter] [surface exchange] [heat used to melt i thickness of ice]

where

$\rho, \rho i$ = density of water, ice

C_p = specific heat of water

a = area (km^2)

d = layer depth

T_W = average upper layer temperature, winter

T_F = average upper layer temperature, fall

ΔH_0 = surface heat exchange

Li = latent heat of fusion of sea ice, and

i = thickness of ice melt.

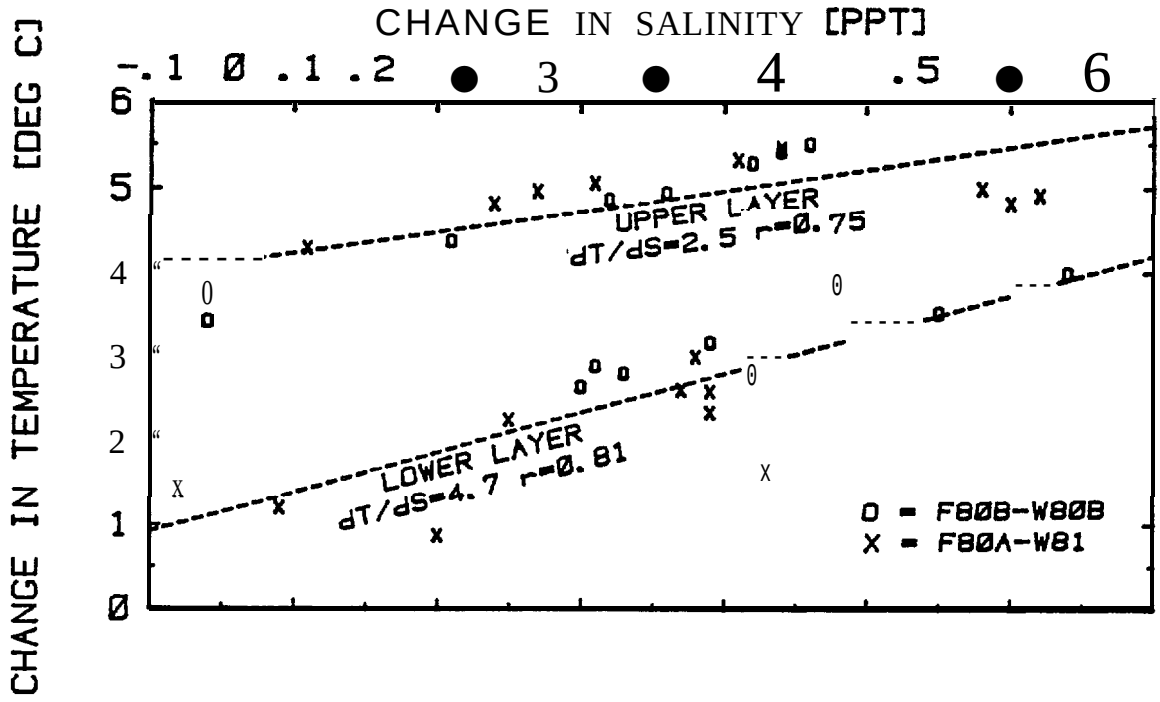

Figure 5.20. Correlation between the temperature and salinity changes within each 25 km interval for the upper layer and the water column from the base of the upper layer to the bottom (average AT and AS) for both comparisons.

The temperature change can be expressed as,

$$AT = T_W - T_F = -\Delta H_0/\rho C_p d - i \left[\frac{\rho_i L_i}{\rho C_p d}\right] \quad (7)$$

For salinity,

$$\rho a d S_F 10^{-3} = \rho a (d+i)\ S_W 10^{-3} \quad (8)$$

where S_F, S_W = average upper layer salinities in fall and winter

$$\Delta S = S_W - S_F = S_F\left(\frac{d}{d+i}\right) - S_F = S_F \frac{i}{d+i} \cong S_F \frac{i}{d} \quad (9)$$

For this expression, the salinity of the melting ice is taken as zero and the layer depth is held constant. Both the temperature and salinity of the upper layer will vary as the amount of ice melt (i). The term ΔH_0, the surface exchange will probably be about constant across the 200 km MIZ.

Combining (7) and (9)

$$\Delta T = - \Delta H_0 / \rho C_p d - \Delta S \frac{\rho i}{\rho} \frac{Li}{C_p S_p} \qquad (10)$$

The slope of the AT - AS correlation in the upper layer should approximately be given by

$$\frac{\rho i}{\rho} \frac{Li}{C_p S_F} \cong 2.4^{o}C/ppt \qquad (11)$$

with

$$\rho i/\rho \cong .9, \; C_p = .94 \frac{Cal}{g\text{-}^{o}C}, \; Li = 80 \frac{Cal}{gm}, \; S_p = 31 \text{ ppt},$$

which is approximately equal to the slope in Figure 5.20. A more detailed derivation of this slope can be found in Gade, 1979. The temperature-salinity changes in the lower layer appear to be correlated but along a steeper slope ($\sim 4.7^{o}C/ppt$) suggesting a different mechanism.

6. DISCUSSION AND CONCLUSIONS

Wintertime hydrographic structure over the southeast and central Bering Sea shelf, based on this 1980-81 data, conforms in many respects to the domains proposed by Kinder and Schumacher, 1981a for the southwestern shelf. During winter over the central shelf, the boundary between the vertically homogeneous coastal domain and the two-layer middle domain appears to occur at about the 75m isobath (Figure 5.13). This boundary may be farther south, over deeper water, than during summer where itis coincident with the 50 m contour. This would suggest that wintertime mixing processes such as due to tides and stirring by the relative movement of ice over the water aided by negative buoyancy addition at the surface by the cooling and freezing process, are able to completely mix the water column to a deeper depth than the summertime combination of wind and tidal mixing. During wintertime the middle domain, with a characteristic two-layer structure, extended from about the 75 m contour to the 100 m contour over the southeastern shelf. Over the central shelf the two layer structure extended seaward of the 100 m contour, to depths of 125 to 150 m.

During winter the temperature and salinity of both the upper and lower layers decrease to the north. Surface layer temperatures remained significantly (>. 1°C) above freezing for distances of 50 to 100 km into the ice pack. The horizontal gradients of temperature and salinity in the upper layer (-2 to -5 x 10-2 °C/km and -6 to -10 x 10^{-3} ppt/km) tended to be greater than the corresponding gradients in the lower layer (-1 to -3 x 10-2 °C/km and -1 to -4 x 10^{-3} ppt/km). The greatest upper layer horizontal property gradients occurred coincident with the approximate position of ice edge (compare Figures 5.10 and 5.11a and b). The horizontal changes in T-S properties were similar along the two central shelf sections ($dT/dS \cong 3$ to 4 °C/ppt). Although both temperature and salinity decrease northward along the sections their effects on the horizontal density gradient are not completely compensating. The reduction in density due to the salinity decrease is greater than the increase in density due to the temperature decrease ($\Delta S/\Delta T \cong 1/4$; $\beta\Delta S/\alpha\Delta T \cong 4$). As a result there is a horizontal density gradient associated with the ice edge which in turn indicates a baroclinic flow in the upper layer directed to the northwest along the ice edge (Figure 5.14).

Fall to winter comparisons can be made by comparing sections W-80B → F-80B and F-80A → W-81. Although changes over the fall to late March period do not reflect total changes in the MIZ over a season, they may reflect some of the important ice-ocean processes and interactions. During fall, the temperatures in the upper layer were in the +2 to +5°C range (Figures 5.1 and 5.4). Upper layer temperatures were a maximum in the south and decreased to the north at about -1×10^{-2} °C/km. Lower layer temperatures were about 1 to 2°C/km lower than in the upper layer and also decreased to the north along nearly the same slope. The salinities along the fall sections (Figures 5.1 and 5.4) also decreased to the north (about 3 to 5×10^{-3} ppt/km) with the lower layer salinities .25 to .5 ppt greater than in the upper layer. Both the vertical temperature (negative) and salinity (positive) gradients were stabilizing. During wintertime the following changes in the temperature and salinity structure were evident. Upper layer temperatures and salinities decreased and the horizontal property gradients increased by a factor of 2 to 4, especially in the region of the ice edge. In the lower layer temperature and salinity also decreased along the sections but significant changes in the horizontal gradients were not so evident. During winter the vertical temperature gradient becomes positive and is a destabilizing component in the vertical density gradient.

The changes in heat and salt content from fall to winter in the MIZ computed for the two comparison sections lead *to* the following conclusions:

- The total change *in* heat content averaged along the MIZ portion of the sections was about 3.7×10^{4} cal/cm^2 (Figure 5.16) of which 60 to 66% occurred in the upper layer and 34 to 40% occurred in the lower layer.
- The total change in salt content averaged along the MIZ portion of the sections was about 2.4 gm/cm^2 (Figure 5.17), equivalent to the melting of 1 m of ice, of which 54 to 56% occurred in the upper layerand44 to 46% occurred in the lower layer.
- Combining the above results with the assumption that the latent heat of fusion for sea ice is about 60 cal/gm suggests that

approximately 15% of the total heat loss is used in the melting of ice and 85% is due to surface exchange (Table 5.2).

- Treating each 25 km interval as an individual estimate of the heat and salt changes given by $\Delta H_{F \to W} = \Delta H_0 + \rho L i$ (Eq. 5) and inputting computed values of $\Delta H_{F \to W}$ and i estimates of AH_o (the intercept) and PL (the slope) were made using regression techniques (Table 5.3) to check the consistency of the observations against this relationship. Correlations were positive and significant at the 5% level for the upper layer cases and two of three of the cases using the total water column. Estimates of the slope, ρL, ranged from 44 to 91 [cal/cm^3] with an average of about 62 [cal/cm^3]; estimates of the intercept, AH_o, were 3.1 x 10^4 [cal/cm^2] for the total water column and 2.0 x 104 [cal /cm^2] for the upper 1 ayer.

- The correlation between the changes in temperature and salinity (Figure 5.20) from fall to winter show a slope, $AT/AS \cong 2.5$ for the upper layer consistent with dilution and cooling by ice melt. The slope for the lower layer, $\Delta T/\Delta S \cong 4.7$ is different suggesting another mechanism, perhaps vertical mixing, may also play a role in determining the lower layer properties.

Both comparisons indicate that by late March about 1 m of ice on the average has melted over a band of 200 km in north-south extent. Using an average thickness of 0.5 m, this equates to a 400 km band of ice advecting south and melting in the MIZ. If southward movement of ice into the MIZ and subsequent melting has taken place over a two month period then the southernly rate of ice movement is about 8 cm/sec. For comparison Muench and Ahlnas, 1976, estimated the southward movement of ice into the MIZ at about 18 cm/sec.

7. REFERENCES CITED

Doherty, B. J., and D. R. Kester. 1971. Freezing point of seawater. J. Mar. Res. 32(2): 285-300.

Gade, H. B. 1979. Melting of ice in sea water: a primitive model with application to antarctic ice shelves and icebergs. J. Phys. Oceanogr. 9(1): 189-198.

Kinder, T. H., and J. D. Schumacher. 1981a. Hydrographic structure over the continental shelf of the southeastern Bering Sea. In The Eastern Bering Sea Shelf: Oceanography and Resources, Vol. I, D. W. Hood and J. A. Calder, eds., 1339 pp.

Kinder, T. H., and J. D. Schumacher. 1981b. Circulation over the continental shelf of the southeastern Bering Sea. In The Eastern Bering Sea Shelf: Oceanography and Resources, Vol. I, D. W. Hood and J. A. Calder, eds., 1339 pp.

Muench, R. D. 1981. Physical oceanographic investigations in the Bering Sea marginal ice zone (draft). SAI/NW-81-250-04, 50 pp.

Muench, R. D., and K. Ahlnas. 1976. Ice movement and distribution in the Bering Sea from March to June 1974. J. Geophys. Res. 81(24): 4467-4476.

Newton, J. L., and B. G. Andersen. 1980. MIZPAC 80A; USCGC Polar Star (WAGB-10) Arctic West Operations. March 1980: Bering Sea. Cruise report and preliminary oceanographic results. SAI-202-80-460-LJ, 32 pp.

Zubov, N. N. 1943. Arctic ice. 491 pp. Transl. USAF Cambridge Research Center, cd., U.S. Navy Electronic Laboratory.